18-cm VLA observations of OH towards the Galactic Centre

Roland Karlsson

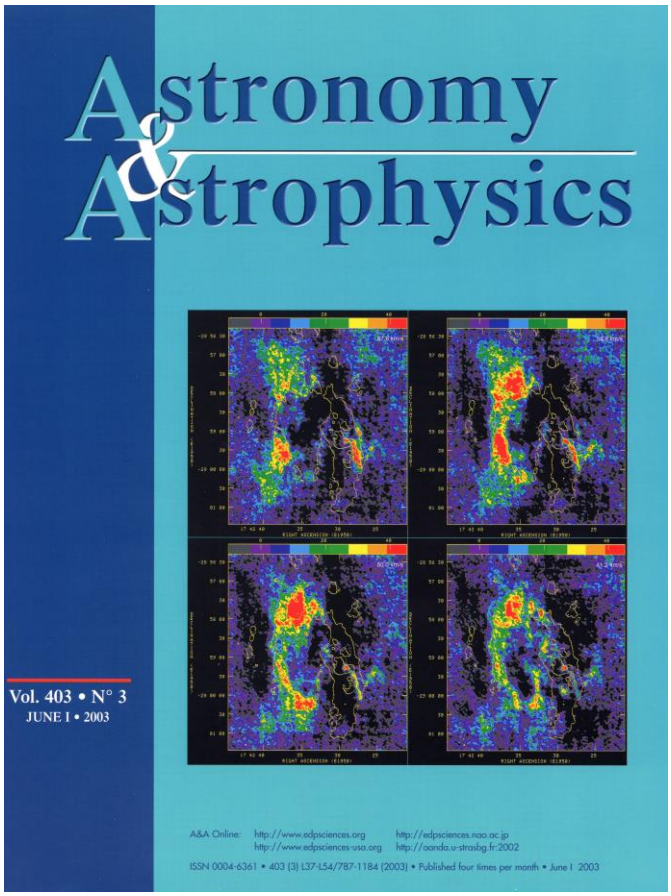

Stockholm Observatory
Stockholm University
2003

Cover image: Cover of Astronomy & Astrophysics Vol. 403, No 3, JUNE I, 2003
OH absorption towards Sgr A in the Galactic Centre
(Karlsson R., et al., p. 1015)

18-cm VLA observations of OH towards the Galactic Centre

Roland Karlsson

Stockholm Observatory
Stockholm University
2003

Licentiate thesis
Stockholm Observatory
Stockholm University
SE-106 91 Stockholm
Sweden

Abstract. The Galactic Centre harbours the enigmatic central energy source of the Galaxy, which by theoretical and deductive methods now is identified as a massive black hole. Its interactions with the near surroundings, which embody a wide range of objects and phenomena – stars, giant molecular clouds, dust, star formation, star collisions, supernovae, etc. – are the tools to understand the processes going on in the boiling centre of the Galaxy and perhaps in other similar galaxies.

The centre of the Galaxy, located at a mere 8 kpc from the Sun, is by far the nearest available nucleus of a galaxy, and a natural candidate for studies of galactic centres. However, the Galactic Centre is visually hidden behind massive obscuring dust clouds, mainly in the vicinity of the Sun, and hence observations are referred to radio-, (sub)millimeter-, IR-, X-ray- and γ-ray wavelengths. Many atomic and molecular species have been identified in the Galactic Centre and their physical and kinematical properties can be investigated by spectral line observations – which are the subject of the present work.

The Hydroxyl (OH) radical distribution in the Galactic Centre has been studied with the VLA, in its extended hybrid BnA and compact DnC configurations. The four transition lines, 1612-, 1665-, 1667- and 1720-MHz, were observed in the BnA configuration, and the main lines, 1665- and 1667-MHz, also with the DnC array. The total velocity coverage was about 550 kms^{-1}, with a velocity resolution of about 9 kms^{-1}, and angular resolutions of $3'' \times 4''$ and $22'' \times 24''$ for the BnA and DnC arrays, respectively. The BnA data cover a region of about 2 arcminutes from the Galactic Centre, while the DnC observations extend to a radius of about 20 arcminutes. The focus of this thesis is on the BnA observations, but the thesis also includes preliminary results of the DnC observations at 1665 and 1667 MHz.

Both absorption and emission features have been studied. The Molecular Belt containing the +20 and +50 kms^{-1} clouds, the Circumnuclear Disk (CND), the High Negative Velocity Gas (HNVG), and a new feature which we call the OH-Streamer were identified in absorption at certain velocities. In addition, 45 point-like maser sources were identified in the four lines, 10 of the masers are new detections.

Preface

The present work presents studies of OH molecular clouds and OH masers in the vicinity of the Galactic Centre. It is based on observations at a wavelength of 18 cm with the Very Large Array (VLA), in June 1986, and October 1989. It is presented as my licentiate thesis in Astronomy, at the Stockholm Observatory at Stockholm University, and is a part of my doctoral dissertation, in preparation.

The thesis is based on the four scientific publications below and on results shown in the Appendix:

I. The 18-cm OH Distribution in the Galactic Center Torus. Aa. Sandqvist and R. Karlsson, J.B. Whiteoak and F.F. Gardner, AIP Conf. Proc. 155, The Galactic Center, ed. D.C. Backer (AIP, New York), p.95, 1987.

II. OH in the Environment of Sgr A. Aa. Sandqvist, R. Karlsson and J.B. Whiteoak; IAU Symp 136, The Center of the Galaxy, ed. M. Morris (Kluwer, Dordrecht), p 421, 1989.

III. Absorption and emission in the Four Ground-State OH Lines Observed at 18 cm with the VLA Towards the Galactic Centre. R. Karlsson, Aa. Sandqvist, L.O. Sjouwerman and J.B. Whiteoak, Astronomische Nachrichten/AN, Suppl. Issue 1/2003.

IV. 18-cm VLA observations of OH towards the Galactic Centre. R. Karlsson, L.O. Sjouwerman, Aa. Sandqvist and J.B. Whiteoak, Astronomy & Astrophysics, Vol 403 No. 3, p. 1011, June I, 2003.

Appendix: Preliminary results of observations with the VLA in its DnC configuration.

Contents

Chapter 1

Introduction

The research field dedicated to the Milky Way, the Galaxy, is a relatively young area of Astronomy. In the end of the 18th century, William Herschel concluded that the Milky Way was an isolated conglomerate of stars and nebulae. He realized that many of the observed nebulae were in fact unresolved stellar systems similar to our galaxy, but also that some were composed of "a shining fluid of a nature totally unknown to us". The general concept of a galaxy was, however, not confirmed until the 1920s, mainly as a result of the extensive observation programs by Edwin Hubble, at Mount Wilson Observatory near Los Angeles. The nature of our galaxy was further advanced in the middle of that decade by Bertil Lindblad, and Jan H. Oort, who developed models for the rotation and large scale dynamics of the Galaxy. The conclusive evidence for the existence of a general absorbing medium in the Galaxy was given in 1930 by R.J. Trumpler.

The Galaxy is a large spiral galaxy possibly with a bar structure. The Galaxy is also characterized as a weak Seyfert galaxy and possesses many of the characteristics of an Active Galactic Nucleus, AGN, except for the evidence of a standard accretion disk and hard UV-spectrum with high excitation emission lines.

The Solar system is located at about 8 kpc from the centre of the Galaxy. Our next neighbour galaxies seem to be the Sagittarius Dwarf Elliptical Galaxy, SagDEG, a small galaxy which is currently in a close encounter with the Milky Way at 15 – 20 kpc, and the double irregular dwarf galaxy, the Magellanic Clouds, orbiting the Galaxy at some 60 kpc. Our nearest large spiral galaxy is the giant Andromeda galaxy, M31, at a distance of about 850 kpc. Due to its relative proximity, studies of the Galaxy and its centre may serve as a tool to reveal and understand a wide range of phenomena in galaxies and in the large scale Universe. For example, the review article by Mezger et al. (1996) has the speaking title: "The Galactic Centre – a laboratory for an Active Galactic Nucleus". Galactic nuclei probably play a crucial role in the energetics and evolution of galaxies, and especially the central engine which produces large amounts of energy for the dynamics of a galaxy. The nucleus of the Galaxy is, however, heavily obscured by the interstellar medium and is not observable by optical means.

In 1932, Karl Jansky discovered that interfering background radio noise was of extraterrestrial origin, and that there was a maximum of intensity with a period of a sideral day in the direction of the densest part of the Milky Way. About a decade later Grote Reber produced the first preliminary radio maps of the sky. However, with their poor resolutions (beams of many degrees) the radio emission that was detected was the extended Galactic background peak near the Galactic Centre. The realization that there is a discrete radio source (Sgr A) at the Galactic Centre was first made by Jack Piddington and Harry Minnett in 1951 (Palmer & Goss 1996), but it was not until in the late fifties that the association of Sgr A with the centre of the Milky Way was generally accepted.

Systematic studies of the Galactic Centre have since the late 1960's been performed at radio wavelengths, and to an increasing extent at infrared, gamma- and x-ray bands in the latest

decades. The improved observing instruments and techniques, both ground-based and on board satellites in orbits around the Earth, have significantly broadened the scientific scope and improved both the quantity and quality of the data. As a result, the number of scientific papers on the Galactic Centre has doubled roughly every three years during the last decade and presently more than one paper a week about the Galactic Centre is published, (Melia & Falcke 2001). Extensive reviews of the Galactic Centre and the massive black hole at the centre have been published by Morris & Serabyn (1996), Mezger et al. (1996) and Melia & Falcke (2001).

The radio band observations aim to study the thermal and non-thermal continuum emission, and specific spectral-line emission or absorption characteristics of the neutral and ionized matter. Further, radio and infrared observations are presently the only ways to infer the character of the ultraviolet radiation field at the Galactic Centre. Studies of the excitation state of the ionized interstellar gas, the continuum and spectral line absorption and emission properties of the neutral and ionized gas species are the tools to perform this.

1.1. The scientific background of the project

Before the advent of radio interferometers, lunar occultation methods were used for obtaining high resolution information of the Galactic Centre, which in this context is defined as the Sgr A radio source and the Giant Molecular Complex, GMC, out to a distance of about 25 pc. For example, Sandqvist (1971, 1973, and 1974) presented an OH absorption line investigation based on the 1968 lunar occultation observations with about 40 arcsecond angular resolution, just enough to resolve some of the discrete features of the Galactic Centre. Whiteoak and Gardner at CSIRO in Epping Australia published in 1975 and 1976 OH line observations made with the Parkes telescope (Whiteoak & Gardner 1975, 1976), and a narrow emission feature was detected in the 1720-MHz transition at +132 kms^{-1}. However, the observation was questioned because no features of similar velocity were known to exist in the line profiles of the other ground-state transitions of OH or transitions for other molecules. Advancing the knowledge further required observations of the OH abundance in the Galactic Centre with higher resolution.

The Very Large Array, which began regular operation in 1980, opened a realm for high resolution radio observations of the Galactic Centre. For example, in 1983, Anders Winnberg at Onsala, performed observations of OH/IR stars with the VLA in a hybrid compact configuration (baselines from 0.1 – 6.9 km) at 1612 MHz, with an angular resolution of about 6", and a velocity resolution of about 1.4 kms^{-1}. A preliminary study of those data by Sandqvist revealed that an extensive mapping with the VLA of the OH absorption at the Galactic Centre would be an interesting and rewarding task. This conclusion is the background and basis for the present project.

The scientific objectives of the full project, of which this thesis is a part, are to:

- Determine the abundance and physical characteristics of OH in the Galactic Centre region.

- Investigate the kinematical properties of the OH molecular clouds in the Galactic Centre region.

- Study the geometric relationship between the OH molecular clouds and the continuum emission at the Galactic Centre.

Serendipitously, 45 point-like OH emission sources were found in the observations of the Galactic Centre and have been studied as an extra benefit.

Chapter 2

The Galaxy – an overview

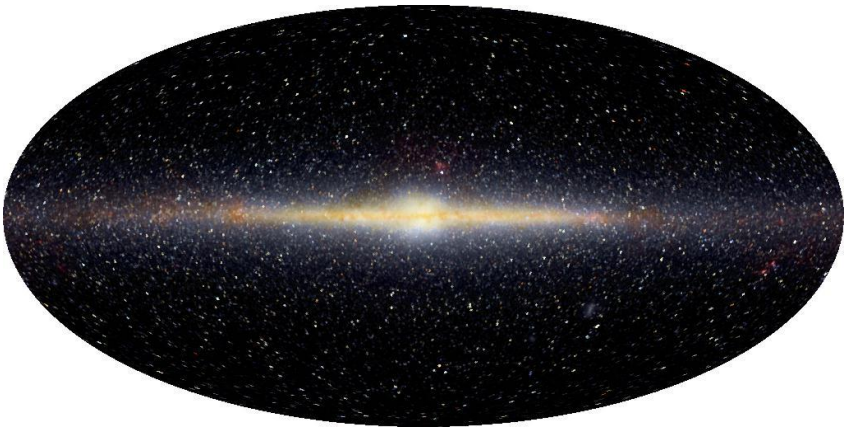

Fig. 1. COBE satellite composite of 1.25, 2.2, 3.5 μm, near-infrared image of the Galaxy (Hauser et al. 1995).

2.1. General

The Galaxy (Fig.1) is a large spiral galaxy in the Local Group of galaxies which contains some forty galaxies. The Galaxy and the Andromeda M31, are the dominant galaxies of the Local Group and account for about 80% of the luminosity of the group.

The total number of stars in the Galaxy is estimated at ~ $2 - 4 \cdot 10^{11}$. The stellar mass in the Galactic Disk (GD), is of the order of ~ $9 \cdot 10^{10}$ $M_\odot$ inside the radius R ~ 14 kpc, and the mass of hydrogen (HI + H_2) in the Galaxy, is estimated at ~ $2 \cdot 10^{10}$ $M_\odot$. About half of the hydrogen is contained in Giant Molecular Clouds (GMCs) (Mezger et al. 1996). The Galaxy is surrounded by a halo of globular star clusters and old stars, including older planetary nebulae, and a dark component of unknown composition with a mass exceeding that of the GD. The GD is probably stabilized by the gravitation of the halo.

The Galaxy is classified as a Hubble type Sb or Sbc by most authors, but the consensus of a bar structure modifies its classification to become a barred spiral of type SB, or intermediate type between barred and "normal" spirals, SAB or SBb or even SBbc, depending on the prominence of the bar.

The morphology of the Galaxy is schematically shown in Fig. 2 (Mezger et al.1996). The direction of rotation is clockwise as seen in the figure, and the Galaxy rotates about its centre at a rate of about one revolution per 200 million year at R ~ 8 kpc. The origin of the spiral structure is thought to be in density waves which are triggered by gravitational disturbances,

in particular during encounters with neighbour galaxies. The density waves compress the interstellar matter, which forms diffuse nebulae which in turn may become star forming regions, and later form (open) clusters and associations of young stars. The Sun, marked by S in the figure, is located in the Local or Orion Arm between two spiral arms close to the Galactic plane. At least one arm even further out and two more inner arms have been identified. The Sun has travelled through the spiral arms and the density waves twenty times or more during its lifetime.
The observed non-circular motion of stars and gas in the central 2 kpc has been interpreted as due to the presence of a bar structure (e.g. Binney et.al. 1991), and the concept of a bar is suggested. The bar is suggested to propel large amounts of gas towards the inner regions of the Galaxy and to modify the velocity field of the stars. The bar model is also used to explain the distribution of molecular emission and absorption and noncircular motions in the 180-pc molecular ring, the so called Expanding Molecular Ring (EMR) (Scoville 1972, Kaifu et al. 1972).

Figure 3 (Mezger et al. 1996) is a zoom picture of the Galaxy and depicts the various components and their approximate geometric dimensions. The sub-picture "d" shows schematically the inner 25 pc of the Galaxy with which this thesis is concerned.

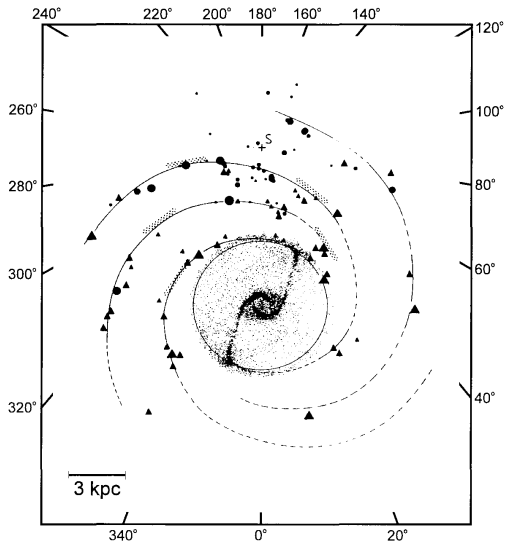

Fig. 2. The morphology of our Galaxy. The spiral structure *R* > 3.5 kpc, is based on observations of Giant HII regions, the central bar structure is based on both radio and NIR observations and model fitting (Mezger et al. 1996).

2.2. The Galactic Disk and Bulge

The Galactic Disk (GD) has a diameter of about 30 kpc. It has a height of about 30 pc in the central region and about 200 pc at the distance of the Sun, $R = 8 \pm 0.5$ kpc (Reid 1993). As seen from the Earth, one arcsecond corresponds to a linear dimension of about 0.04 pc at the Galactic Centre or ~ 0.13 light years. The GD consists of young Population I and very old Population II stars, and an interstellar medium of gas and dust. A layer of gas and dust is concentrated to the Galactic plane. Stars are being formed throughout the GD. A region between $R = 1.5$ kpc and 3 kpc, is markedly devoid of interstellar medium (see Fig. 3). The Galactic Bulge extends to about $R = 1.5$ kpc from the centre, and is composed mainly of Population II stars.

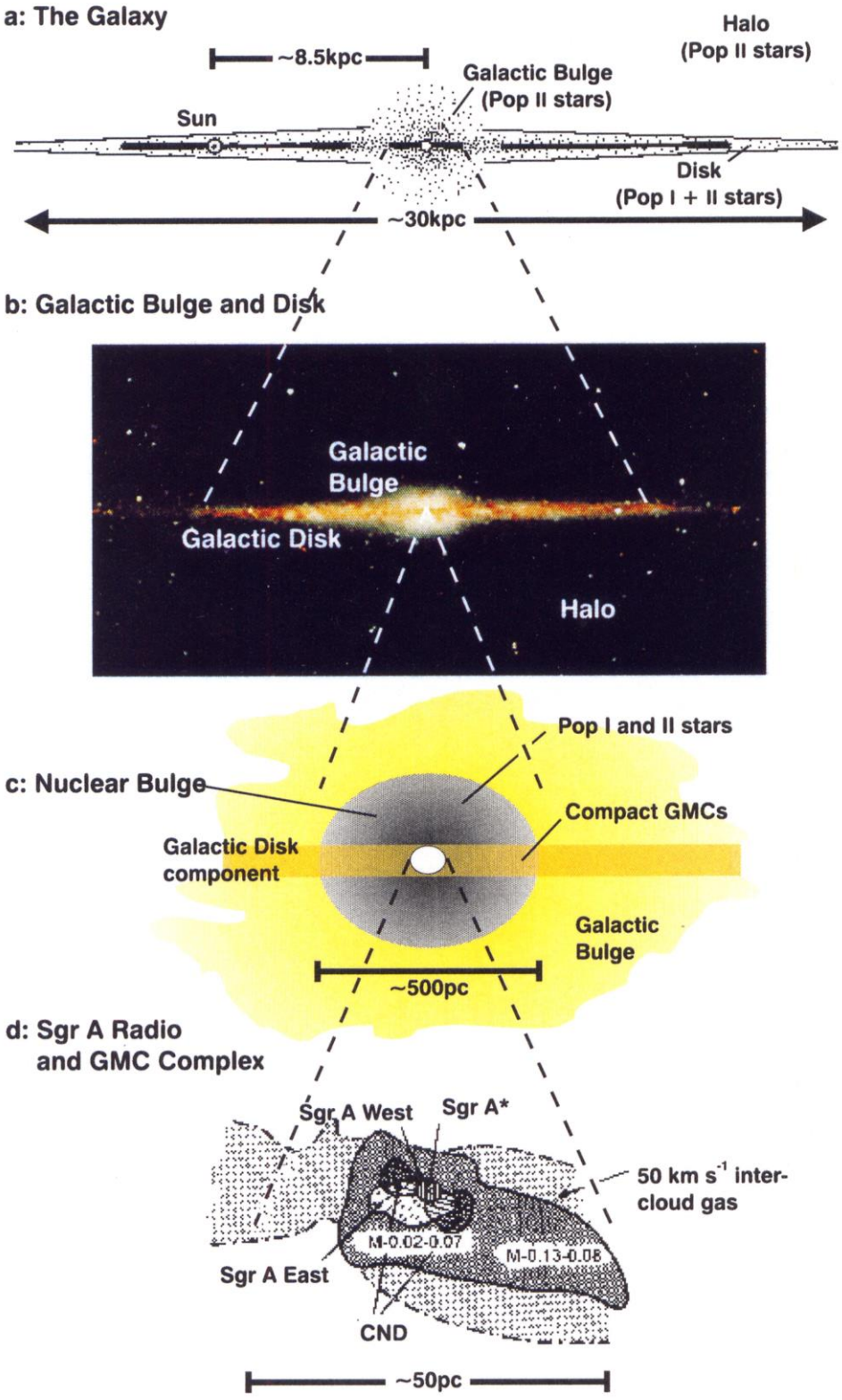

Fig. 3. A zoom picture of the Galaxy (Mezger et al. 1996).

2.3. The Central Molecular Zone, CMZ

Half of the molecular gas in the central 600 pc is contained in very compact giant molecular clouds GMCs, each of a mass of $10^4 - 10^6$ $M_\odot$, average densities of $\geq 10^4$ cm^{-3} and gas kinetic temperatures in the range of 30 – 200 K, with typical values of ~ 70 K (Hüttemeister et al. 1993). The interstellar medium comprises some 10% of the mass of the central 300 pc of the Galactic Centre. In general, the magnetic fields are strong and the field lines are oriented parallel to the Galactic plane inside the GMCs, and perpendicular to the plane in the intercloud medium.

A mixed molecular and atomic tilted layer occupies the region inside the "3-kpc arm". A strong concentration of gas, the Central Molecular Zone (CMZ) with a radius of about 200 pc, is characterized by large densities, large velocity dispersions, high temperatures and apparently strong magnetic fields (Morris & Serabyn 1996). The structure of the CMZ is best delineated by the high-resolution observations of the CO molecule seen in Fig. 4, (Morris & Serabyn 1996). The CMZ is inside the 3-kpc arm and, at a radius of about 200 pc, a transition occurs to a largely molecular medium with a high density of about $n \geq 10^4$ cm^{-3}. The CMZ contains ~ $5 - 10 \cdot 10^7$ $M_\odot$ of gas (Armstrong & Barrett 1985).

The physical state of the gas and the resultant star formation processes in this area are quite unlike those occurring in the large-scale disk. The temperature, pressure, velocity dispersion and magnetic field strengths are all very much larger than in the GD. Strong tidal forces, overcoming the clouds´ self-gravity, may reduce the star formation rate, or even prevent stars from forming near the nucleus, and hence only the densest clouds are capable of making stars in this area. However, in the unusually dense and massive cloud, Sgr B2, (~ 10^8 cm^{-3}, ~ $3 \cdot 10^6$ $M_\odot$) located about 0.7˚ (~ 100 pc) from the Galactic Centre (Figs. 5 and 6) stars are formed at a very high rate. The formation of stars is likely to be triggered by events external to the clouds, like cloud collisions, supernova remnants, and violent gas outflows from the Galactic nucleus.

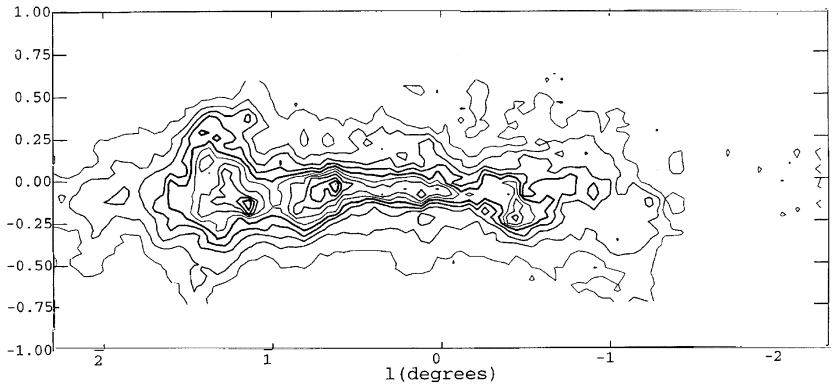

Fig. 4. Our Galaxy's central molecular zone, integrated intensity of ^{12}CO, $J = 1 - 0$ emission (Morris & Serabyn 1996).

The clouds in the CMZ generally show high temperatures, typically ~ 70 K (Güsten et al.1981). Such high gas temperatures and the observed internal velocity dispersions of ~ 15 – 50 kms^{-1} are indicative of a widespread heating mechanism. The best candidate for the heating of the CMZ is dissipation of turbulent energy (Wilson et al.1982).

On the basis of the molecular kinematics of the zone, the CMZ gas can be divided into two components, a high velocity (130 – 200 kms^{-1}) quasi-continuous ring with a radius of about 180 pc, the Expanding Molecular Ring (EMR), and inside this boundary a second massive molecular population of dense massive cloud component with a lower velocity (≤ 100 kms^{-1}).

The EMR is tilted relative to the Galactic plane and probably marks the location of a transition of HI/H_2 (Binney et al.1991). The cloud family inside the EMR includes features associated with Sgr A, and is close to the Galactic plane and is referred to as the "disk population" of clouds. This disk population also contains filament-like clouds with coherent velocity gradients over scales of 30 – 100 pc, suggesting tidally stretched arcs or arms of dust lanes. Several of these features are very massive, for example the Sgr B2 complex, which is the most massive known molecular cloud in the Galaxy, containing about 5% of the gaseous mass in the CMZ. Another handful of large clouds contributes to up to one third of the CO flux of the CMZ. The true geometric arrangement of these clouds still remains ambiguous, but kinematics suggests that the gas is flowing in a barred potential. The distributions of both ionized gas and diffuse infrared emission in the CMZ are more symmetric than the CO distribution (Fig. 4), suggesting that heating sources are more evenly distributed than the discrete clouds.

2.4. The Diffuse Hot Gas

Embedded in the central part of the CMZ is a region of diffuse X-ray emission, with a dimension of about 1.8° x 1.0° (Predehl & Trümper 1994) i.e. ~ 250 × 150 pc of projected size. The apparent linear size of this feature and its sound speed indicate an age of ~ $5 \cdot 10^4$ years, (Koyama & Maeda 1996). This region is most clearly outlined in the intense 6.7 keV Kα transition of He-like iron detected by the Ginga satellite and reveals the existence of a high temperature plasma (Fig. 5). The iron-line emission is consistent with its production by a shock-heated plasma produced by an energetic explosion (Koyama et al. 1989, Koyama & Maeda 1996).

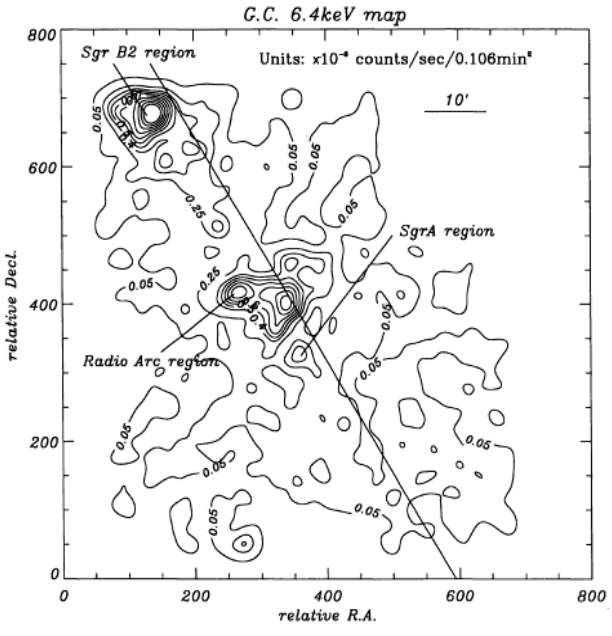

Fig. 5 . Brightness distribution of the 6.4 keV line, obtained by ASCA (Koyama et al. 1996).

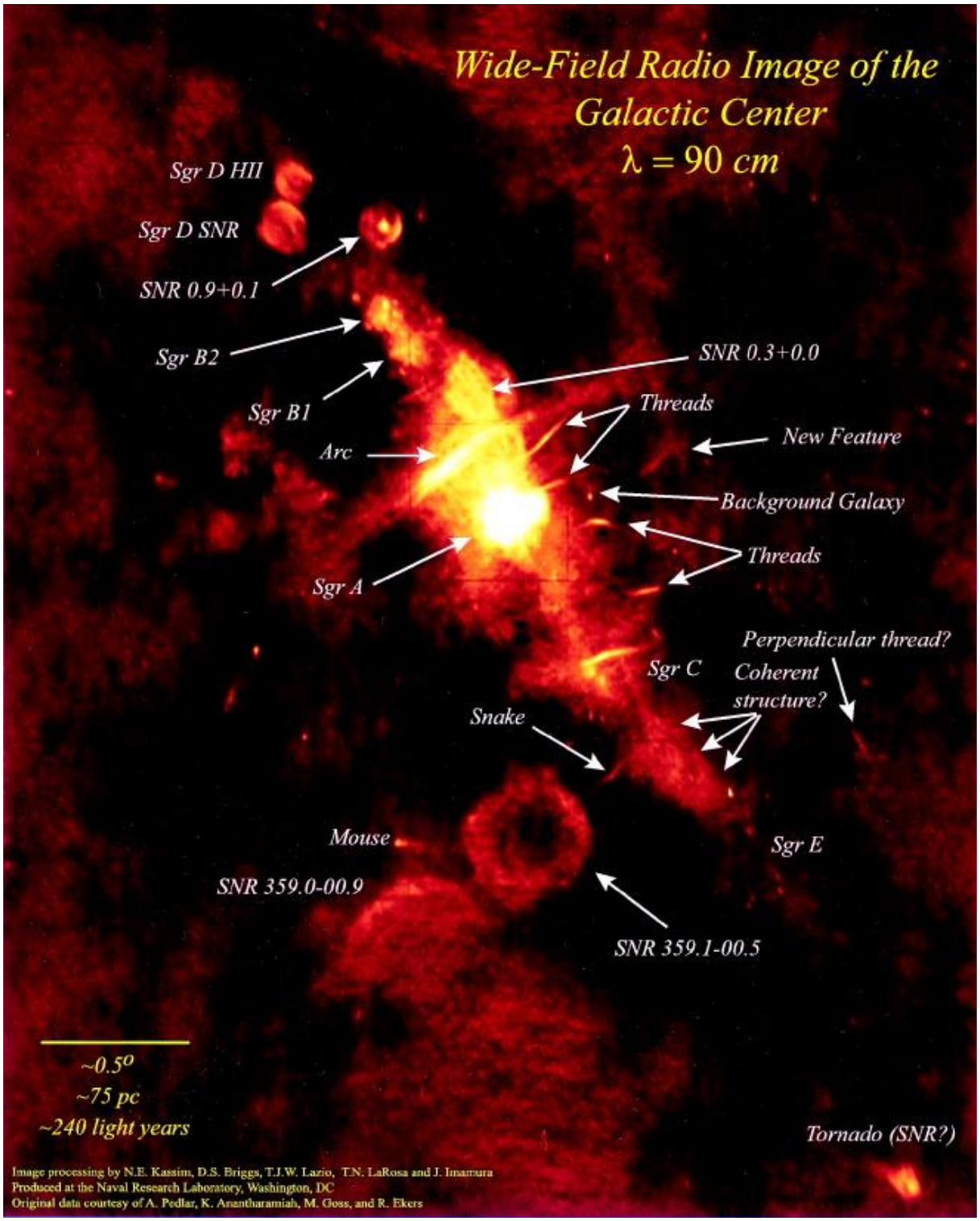

Fig. 6. The 90-cm continuum emission from Galactic Centre. This is a 4° × 2°.5 subimage with a resolution of 43" × 24" and an rms sensitivity of 5 mJy beam^{-1} (NRL, Washington, DC 2002).

Chapter 3

The Galactic Centre at $R \leq 50$ pc

The Galactic Centre (GC) is hidden behind about 30 magnitudes of visual extinction. Visible and ultraviolet observations of the GC are therefore ruled out. The bulk of the extinction is believed to be the result of clouds and dust within 4 kpc of the Earth, and not due to clouds within the inner few parsecs of the Galaxy (Sanders et al. 1985). Most of the existing information about the GC region is gathered from observations at radio, (sub-)millimetre and infrared wavelengths, and to an increasing extent from the X-ray and gamma-ray bands. With the help of radio interferometers, it is possible to study the stars and the components of the interstellar medium in the GC at angular resolutions down to tenths of an arcsecond, i.e. at projected linear scales of 0.004 pc or some 800 AU (~ $1.2 \cdot 10^{16}$ cm).

The region around the GC harbours a variety of phenomena like star formation, star collisions, supernovae, gas and dust clouds and streamers, magneto-hydrodynamic flows, accretion and expulsion of matter, etc. in connection with a massive black hole. Figure 6 shows a number of prominent features and their commonly referred names. Interactions between these components are probably important for the structure and evolution of the Galaxy. Similar processes probably also exist in other galaxies of similar type, and in the same phase of evolution. Stars, possibly with the exception of the innermost parsec, dominate the mass in this region and out to a distance of about 100 pc from the GC.

A relatively new approach of revealing star-forming sites is the study of masers, since H_2O, SiO and the OH masers at 1612, 1665 and 1667 MHz can be used as probes for star formation areas. In evolved late-type OH/IR stars of different masses, i.e. ages, 1612-MHz OH masers are generated in their circumstellar shells during a short-lived phase of heavy mass-loss. In addition, OH maser emission at 1720-MHz is recently found to be a diagnostic tool of interaction between SNR´s and surrounding molecular clouds (Frail et al. 1994). OH is collisionally pumped by H_2 molecules at the site where C-type supernova shocks drive into adjacent molecular clouds (Yusef-Zadeh et al. 1998, Yusef-Zadeh 1999). As a result of this thesis Karlsson et al. (2003), Paper IV, present observations of 45 OH masers at all four frequencies.

3.1. The Molecular Belt and the Sgr A Radio Complex

Figure 7 shows the 1350-μm dust emission from the Molecular Belt, which stretches in a northeast-southwest direction across the Sgr A Complex. It also shows the 2.2-μm emission from the central star cluster – note the absorption from the dust in the Molecular Belt in the 2.2-μm emission. The Molecular Belt includes the +50 kms^{-1} (M–0.02-0.07) and +20 kms^{-1} (M–0.13-0.08) cloud condensations, and it appears that the +50 kms^{-1} and +20 kms^{-1} clouds actually represent the same GMC.

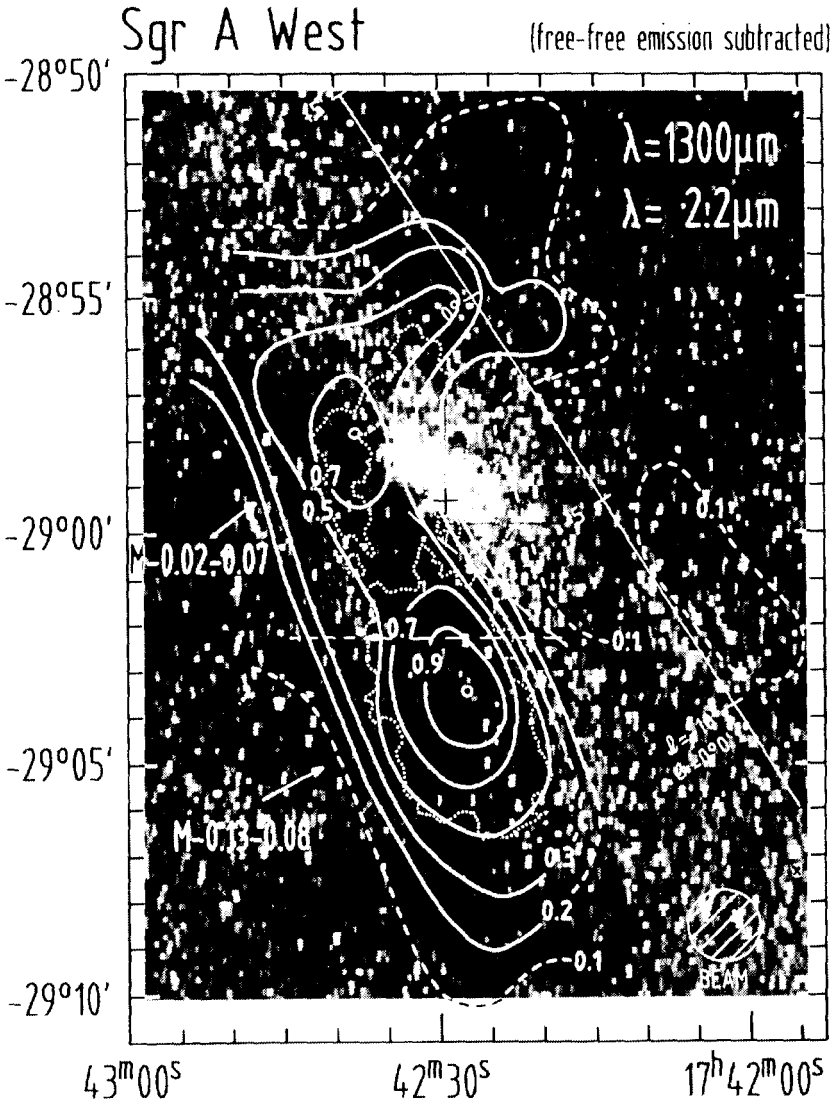

Fig. 7. A λ1.3 mm dust emission contour line image (θ_A ~ 90") is overlaid on a λ2.2 μm grey scale image (Δα × Δδ ~ 6" x 12"). The peak NIR surface brightness indicates the central stellar cluster. The cross marks the position of the compact synchrotron source Sgr A*. The dust emission from the +50 kms^{-1} (M-0.02-0.07) and +20 kms^{-1} (M-0.13-0.08) clouds are seen as condensations in the Molecular Belt running approximately parallel to the Galactic Plane (Zylka et al. 1990).

The Sgr A Radio Complex is the intense continuum radio source of ~ 30 pc size. The continuum source components are: the Arc and the Bridge, the Sgr A halo, the non-thermal (synchrotron) source Sgr A East, the thermal "mini-spiral" Sgr A West, the non-thermal compact source Sgr A*.

Figure 8 is an extract of the concatenated BnA and DnC data set of the present observations, and it shows clearly the inner components of the Sgr A Complex: Sgr A East, Sgr A West, and the HII regions apparently lying close to the edge of the expanding shell of Sgr A East. It is intriguing to assume that the shock wave compressing the +50 kms^{-1} molecular cloud has provoked the formation of the stars that ionize the HII regions. However, the time scale for expansion of the shell is significantly shorter than for star formation and evolution into the main sequence, and the origin of the HII regions is not yet understood, (Morris & Serabyn 1996). A result of this thesis is that Karlsson et al. (2003), Papers III and IV, report that there

is no OH absorption against the HII regions at the velocities of the Molecular Belt and conclude that the HII regions are located on the near side of the +50 kms^{-1} cloud.

The region of the inner $R \leq 25$ pc of the GC contains six principal components: a remnant of a powerful explosion, a molecular and dusty ring or disk, ionized and neutral gas streamers, diffuse hot gas, a cluster of evolved and young stars surrounding the central radio source and the source itself – Sgr A* with the massive object at the centre, the massive black hole.

3.2. Remnant of a powerful explosion – Sgr A East

The Sgr A East shell is, together with Sgr A* and Sgr A West, the brightest continuum source in the GC. The shell has a size of ~ 7 × 9 pc, with its centre at a projected distance of ~ 2.1 pc from Sgr A*.

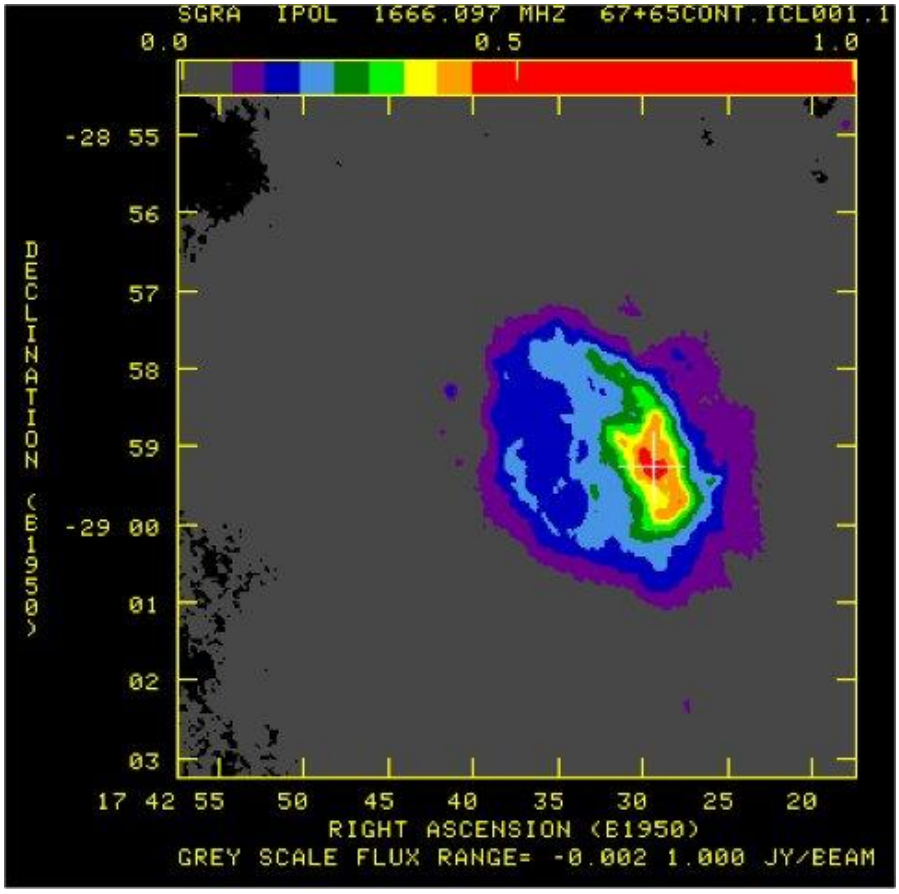

Fig. 8. The Sgr A Complex in the 18-cm continuum, showing the Sgr A halo (violet), the Sgr A East shell (blue), the Sgr A West minispiral (amber and red) and the string of compact HII regions to the east. The position of Sgr A* is marked by a white cross. Preliminary concatenated data from observations with the VLA BnA and DnC configurations (Karlsson et al. 2004, in preparation).

Based on observations and model fitting, Yusef-Zadeh & Morris (1987) concluded that Sgr A East is the remnant of an explosive event which occurred inside the Sgr A East shell ~ $6 \cdot 10^4$ years ago with an energy output of ~ 40 supernovae which ruled out a "normal" supernova explosion with a typical energy output in the order of ~ 10^{51} erg. X-ray observations also indicate a common source of origin for the entire plasma in the inner ~ 150 pc, rather than a superposition of a number of individual sources such as supernovae, since the brightest objects in Fig. 5, the Sgr B2 cloud and a region of high intensity north of Sgr A* in the area of the Bridge and the Arc, have similar spectra. Assuming an expansion velocity equal to the sound speed one obtains an expansion age of ~ 10^5 yr, comparable to the age of the Sgr A East and the Circumnuclear Disk (CND) surrounding Sgr A West (Mezger et al. 1996). The explosion may have affected the structure of the CND and Sgr A* itself was probably also hit by the shock waves. This model has in later papers gained support by Mezger et al. (1989) and others. Yusef-Zadeh and Morris also showed the existence of a diffuse radio structure around Sgr A East and Sgr A West with a diameter of about 20 pc. This halo is also associated with a set of narrow radio "threads" roughly perpendicular to the Galactic plane (see Fig. 6). Some of the threads are seemingly connected to Sgr A West. Mezger et al. (1989) detected a ~ 10-pc diameter ring of molecular gas surrounding the Sgr A East shell (Fig. 9). At its eastern edge the shell is compressed while gas with both positive and negative velocities is present at the northwestern edge, possibly indicating that the core is disrupted in this area. The total mass of the dust ring is estimated at ~ $6 \cdot 10^4 \, M_\odot$.

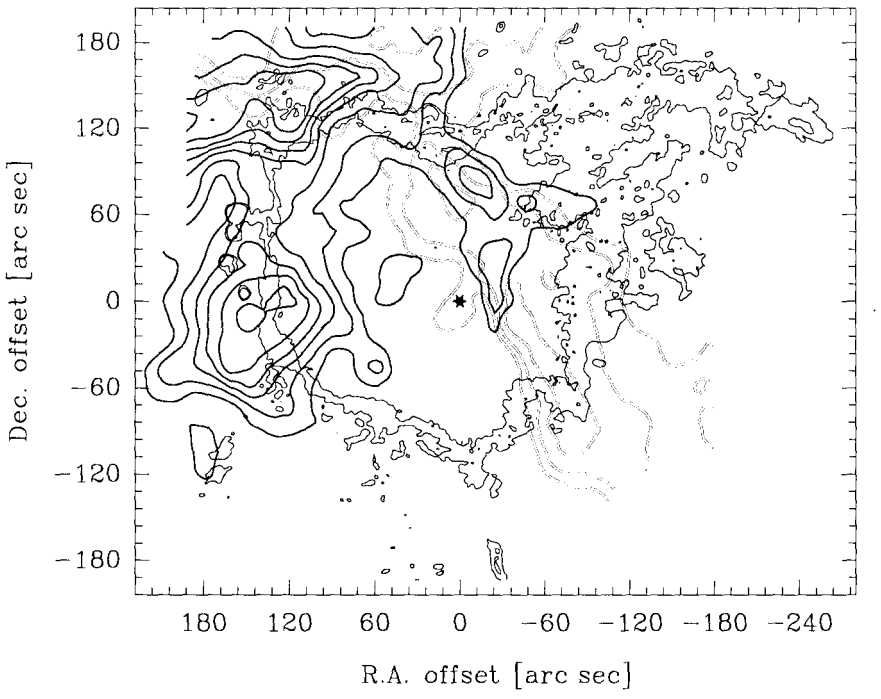

Fig. 9. ^{13}CO(2-1) emission integrated over the velocity interval $-20 < v < -10$ kms^{-1} (double lined contours) and $+60 < v < +100$ kms^{-1}. The thick solid contours outline the eastern part of the Sgr A East Core, while the solid and double-lined contours outline the disrupted northern and western part of this cloud. The λ6-cm continuum emission is shown for reference as thin contours (Mezger et al. 1996).

3.3. The molecular and dusty ring – the CND

The most prominent molecular feature in the central parsecs of the GC is the CND, with a radius of about 1 pc. It is a dense ring or torus-like centrally illuminated clumpy structure that orbits around Sgr A* (Figs. 10 and 11). It is not clear whether the CND should be considered as a coherent ring structure or separate clumps or clouds comprised of debris material, although the latter explanation seems to gain support. For example, HCN observations by Jackson et al. (1993) indicate that the CND consists of several kinematically distinct streamers. Furthermore, the large interclump velocity dispersion points to frequent clump-clump collisions and shocks (Marshall & Lasenby 1994). The inward facing surfaces of the molecular material seem to be photo-ionized in the parts of the CND that are close to Sgr A*. The ionization is mainly from the central cluster of stars, and locally by individual stars (Aitken et al. 1990). The gas in these areas is hot (a few hundred K) and dense (10^4 – 10^7 cm^{-3}), and comprises line emission consistent with a photo-dissociation region (Genzel et al. 1994). The appearance of the CND indicates a dynamical time scale of ~ 10^5 yr (Güsten et al. 1987).

The typical velocity of rotation is ~ 100 kms^{-1} in the same general direction as that of the Galaxy itself. The inclination of the CND is ~ 20 – 30°, if assumed intrinsically circular. The area inside of the CND is referred to as the Central Cavity, and contains Sgr A West and Sgr A*, but is otherwise swept clear of matter by outflow winds (Gatley et al. 1984, 1986). The molecular medium extends in general only to about 1.5 pc from the centre with an inner sharply defined ionized boundary layer. Much of the filamentary structure of Sgr A West is located inside of 1.5 pc. A result of this thesis is that Karlsson et al. (2003) Paper IV, estimate the enclosed mass within about 1.84 pc from Sgr A* to be at least 7.5 $\cdot 10^6$ $M_\odot$, based on observations of 1720 MHz OH masers in the CND and thus ~ 50% of this mass consists of an enclosed stellar cluster and molecular gas assuming a mass of 3.7 $\cdot 10^6$ $M_\odot$ for the central object (Schödel et al. 2002). The CND and its observed components are further discussed in Karlsson et al. (2003) Paper IV.

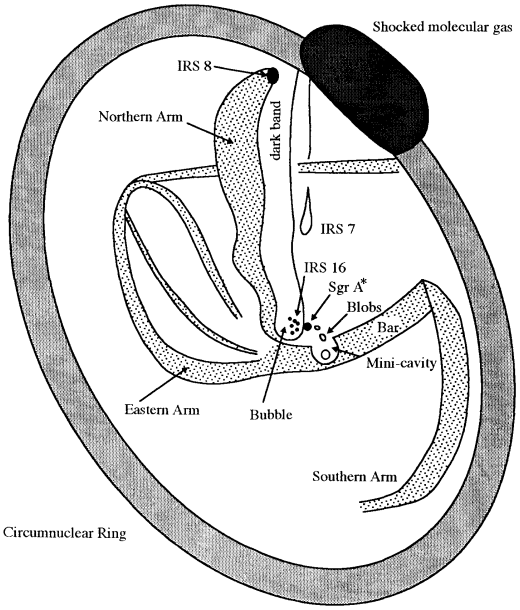

Fig. 10. A schematic diagram showing prominent features (CND, Sgr A West and Sgr A*) of the inner two parsecs of the Galaxy (Yusef-Zadeh & Wardle 1992).

There is evidence for a large-scale magnetic field configuration within the CND from polarization measurements of 100-μm dust emission by Werner et al. (1988) and Hildebrand et al. (1990). Observations of the Zeeman-splitting of HI and OH lines indicate a magnetic field strength of 2 mG in the southern part of the CND and a marginal detection in the northern part (Schwarz & Lasenby 1990, Killeen et al.1992). The energy density of the magnetic field in the CND is thus about 10^{-7} erg cm^{-3}, while that of the large-scale rotational and non-circular motion is about 10^{-5} erg cm^{-3} or more.

The net mass flow from the CND towards the GC is probably best described in terms of sporadic infall of individual clumps resulting from inter-clump collisions, or tongues of gas spitting off the inside of the CND as a result of instabilities at this surface. The inflow rate of interstellar matter from the CND into the Central Cavity is estimated at ~ $3 - 5 \cdot 10^{-2}$ $M_{\odot}$ yr^{-1} (Güsten et al. 1987, Jackson et al. 1993).

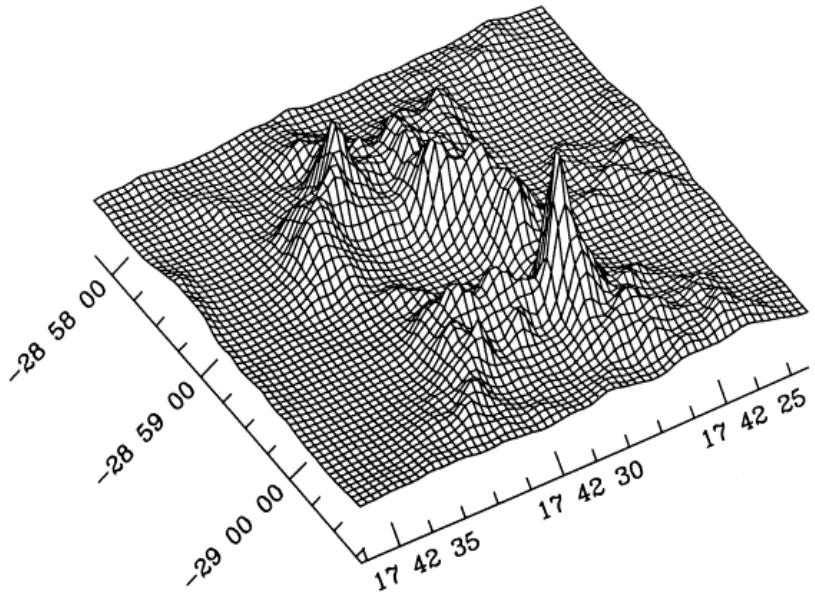

Fig. 11. Relief representation of the CND in the HCN line, velocity integrated $-150 \leq v_{LSR} \leq +150$ kms^{-1} (Güsten et al. 1987).

A result of this thesis is the discovery of a streamer of gas that appears to have enough inertia to penetrate the Central Cavity region and survive in the intense UV- radiation field – the "OH-Streamer" – (Sandqvist et al. 1987, 1989; Karlsson et al. 2003 Papers III and IV). The OH-Streamer seems, in projection, to stretch from the southwestern part of the CND, through the Central Cavity, and pointing to the radio source Sgr A*. The OH-Streamer is detected between velocities of about –20 kms^{-1} and +68 kms^{-1}, and the main direction of the streamer seems to turn in a counterclockwise direction as it approaches Sgr A* (Fig.12). However, the velocity of the OH-Streamer in the region of the CND differs by more than 100 kms^{-1} from that of the CND, which may indicate that the OH-Streamer is not in the same plane as the CND.

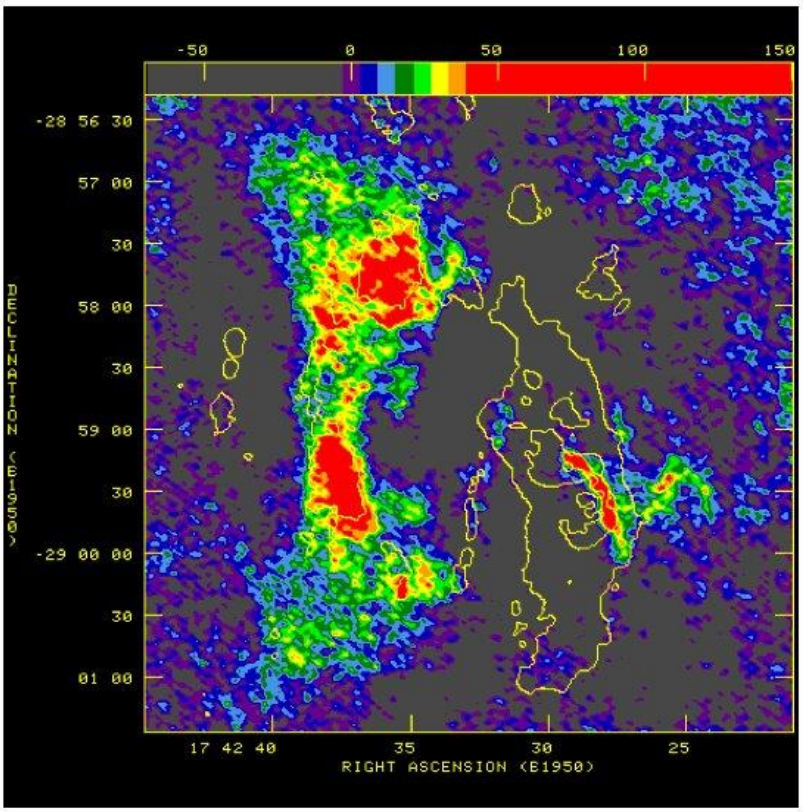

Fig.12. The 1667-MHz OH absorption at +58.8 kms^{-1} towards Sgr A, a thesis result. Note the OH-Streamer near Sgr A*and the absorption towards Sgr A East. The continuum emission is indicated by the contours: 15 mJy/beam indicates Sgr A East and the compact HII-regions to its east, 93 mJy/beam indicates Sgr A West and 500 mJy/beam indicates Sgr A*.

3.4. Ionized and neutral gas streamers - Sgr A West

Sgr A West is a basically three-arm spiral configuration of ionized gas and dust. It was first separated from the synchrotron source Sgr A East by Sandqvist (1971, 1974). The different parts of this HII region are referred to as the Minispiral with the Northern and Eastern Arm, the central Bar, the Western Arc (Fig.13). Lo & Claussen (1983), Ekers et al. (1983) and Roberts et al. (1996) suggest from observations the following model for Sgr A West: The Western Arc is the ionized inner edge of the CND, both the northern and Eastern Arms are tidally stretched ionized streamers which transport mass towards the centre, and the Bar could be an extension of the Northern Arm. Between the Northern and Eastern Arms there is a concentration of neutral atomic gas observed in the OI line, between radial velocities of ~ 30 to 75 kms^{-1}. The gas appears to fall in from the north towards the central parts of Sgr A West and is referred to as the "Tongue" or the "Northern Intruder". The mass of the Tongue is estimated at ~ 300 $M_{\odot}$ and it is suggested to feed material from the surrounding GMCs into the GC with the Northern and Eastern arms representing the ionized interfaces (Jackson et al. 1993). Furthermore, Serabyn et al. (1988) and later authors suggest that Sgr A West is rotating around Sgr A* in a counterclockwise direction at a velocity of about 150 kms^{-1}. A striking feature of Sgr A West is also the "minicavity", centred near the junction of its Northern and Eastern Arms. It is a distinct "hole" in the radio continuum emission, with a diameter of about 2″, corresponding to ~ 0.08 pc. Sgr A West is probably ionized from the central distribution of bright stars, rather than from the point source, Sgr A* (e.g. Zylka et al.1995).

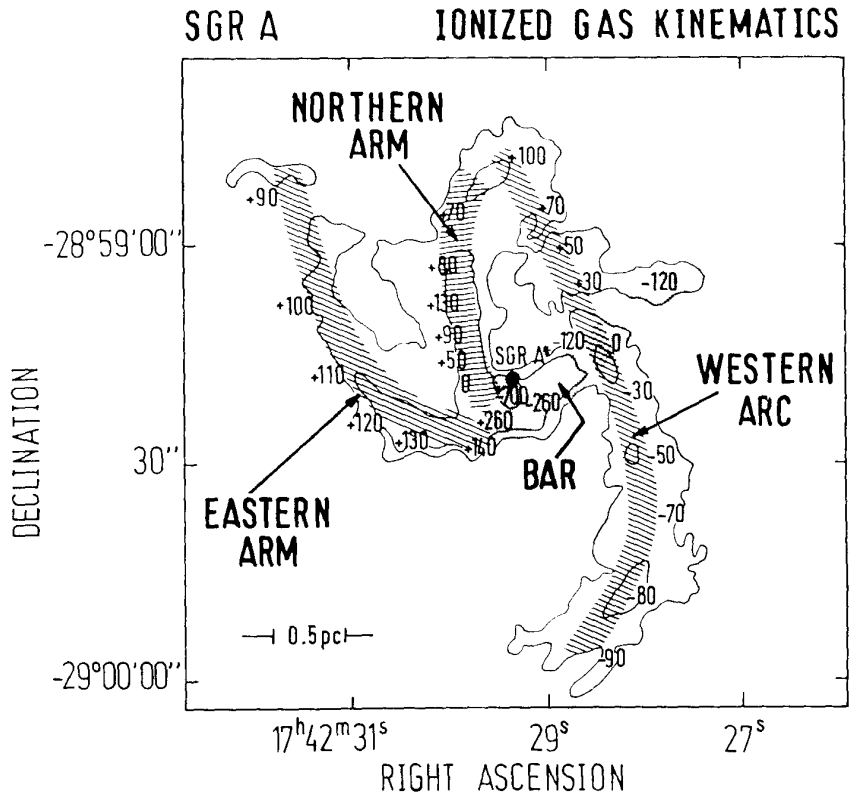

Fig. 13. Overview of the ionized velocities superposed on the Lo and Claussen (1983) 6-cm continuum map. The measurements in the Western Arc, Bar, Northern and Eastern Arms are from 12.8-µm[NeII] spectroscopy by Lacy et al. (1980) and Serabyn & Lacy (1985), and from H76α recombination line measurements by Schwarz et al. (1989). The ±700 kms^{-1} broad line emission region is from 2-µm He/H spectroscopy by Hall et al. (1982) and Geballe et al. (1984, 1987).

3.5. The High Negative Velocity Gas, HNVG

The High Negative Velocity Gas (HNVG) was detected in H_2CO by Güsten & Downes (1981) at velocities around –180 kms^{-1}. The gas has also been observed in OH and HI in absorption against Sgr A East and West (Zhao et al. 1995). The HNVG is well centred on Sgr A* which is indicative of a physical association with the GC. Zhao et al. argue that the HNVG is well mixed with the ionized gas in the GC and that the observed kinematics is not consistent with ejection, outflow or a possible association with the EMR. Zhao et al. also suggest that the Minicavity 3" southeast of Sgr A* could be the result of an impact of a high velocity streamer.

Based on the similarity of kinematics with the ionized gas surrounding the Minicavity and on model calculations a close association between the HNVG and Sgr A West is suggested. This conclusion is supported by observations by Genzel et al. (1996) that the early-type stars in the central 5 – 10 arcsec rotate in a direction opposite to the general Galactic rotation. Genzel et al. suggest that the early-type stars were formed at a single epoch $\sim 3 - 9 \cdot 10^7$ years ago, when a counter-rotating dense and massive cloud lost angular momentum by collisions with regularly rotating clouds and fell into the central parsec.

A result of this thesis is that Karlsson et al. (2003) Paper IV observe that the HNVG located northeast and southwest of Sgr A*, between about $-223 \leq v_{LSR} \leq -160$ kms^{-1}, is double-lobed and has a maximum intensity around –170 kms^{-1}.

3.6. The cluster of evolved and young stars surrounding Sgr A*

The central parsec of the Galaxy holds a mixture of young and evolved stars. The early type stars are concentrated in the central ~ 12 arcseconds (Genzel et al. 1996). IRS 16 is the brightest central condensation of this cluster of early type stars. On the other hand the brightest later type stars, red supergiants and AGB stars, seem to avoid the central 4 arcsec and form a ring which peaks at about 7 arcsec. This ring appears to delineate the region of recent high-mass star formation. The early type stars in the central 5 – 10 arcsec rotate in a direction opposite to the general Galactic rotation (Genzel et al. 1996). The spatial distribution of low-mass main sequence stars is not known, since they are too weak to be detected in the NIR-images, although they most likely dominate the stellar mass distribution in this region.

Gas not consumed by star formation either enters a hot X-ray emitting halo and is lost as a thermally driven galactic wind, or continues moving inward through the domain of the few parsec-sized clumps and into the central parsec, according to the massive Black Hole/Accretion Disk (BH/AD) model for the "Central Engine" (Fig.14, Begelman et al. 1989). Inflow of material is observed in the Nuclear Bulge on all distance scales. The inflow is primarily in the Galactic plane and amounts to a few 10^{-2} $M_\odot$ per year.

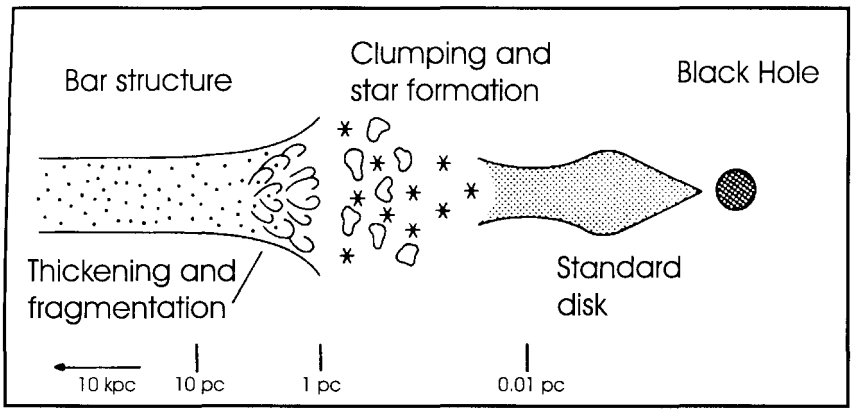

Fig. 14. Schematic presentation of the Massive BH/AD model for the "Central Engine", from Begelman et al. (1989).

There is evidence of recent, $3 – 7 \cdot 10^6$ years ago, massive star formation in the central parsec (e.g. Lebofsky & Rieke 1982). The central parsec of the GC also seems to be the site of repetitive bursts of star formation, fuelled by the radial inflow of gaseous matter, although the inhibiting factors to star formation – tidal forces, cloud turbulence, magnetic fields – are extreme in the central parsec. The initial conditions for star formation in the GC differ greatly from those found at other locations in the Galaxy. The temperature, pressure, velocity dispersion and magnetic field strengths are all much larger in the CMZ than in the GD. Consequently, star forming events in this area must be unusually violent and it seems likely

that much of the star formation is induced by events external to the clouds, like shocks associated with cloud collisions, supernova remnants and perhaps violent outflows from the nucleus (Morris & Serabyn 1996). The gas not consumed by star formation may stream inward (Fig. 14) through a region of parsec-sized clumps as well as through the CND, and eventually end up in the central parsec of the GC or onto an accretion disk surrounding the massive black hole at the centre. Recent observations support the idea of a mass inflow rate varying with time (Mezger et al. 1996).

For the central 1.5 pc the gravitational potential is dominated by the central compact mass, while at radii $R \geq 1.5$ pc, the gravitational potential is dominated by the central star cluster (Genzel & Townes 1987). See also Sect. 3.3.

The effect of winds has been demonstrated for the cluster of young and evolved stars within the central parsec. The GC wind appears to be produced by the early-type stars enclosed within the Western Arc, the Northern Arm and the Bar (Coker & Melia 1997). The 1.5-pc radius Central Cavity inside the CND may be the result of mass outflow winds sweeping the area clear from gas. High-resolution observations of NeII- and optically thick continuum emission at 2 and 6 cm from IRS 7, a cool red supergiant star located at a projected distance roughly 3 pc from the GC, show a remarkable tail of ionized gas pointing directly away from Sgr A* (Serabyn et al. 1991, Yusef -Zadeh & Morris 1991). The tail is interpreted in terms of the ionization and removal of the circumstellar envelope of the red supergiant either by the ram pressure of the nuclear wind or by the pressure of radiation arising from the immediate vicinity of Sgr A*. Furthermore, a cluster of about 100 massive stars resides at $0.2 \leq R \leq 0.3$ pc, giving rise to stellar winds and production of X-ray emission (C. Law at the GC Conference, 2002).

3.7. Sgr A*, and the massive object at the centre – the black hole

The nature of the central energy source is of fundamental interest, and principally two candidates exist: a dense cluster of giant stars or a massive black hole. The idea of a massive black hole was first pointed out by Lynden-Bell & Rees (1971), and the evidence for the existence of a dark mass concentration has steadily grown since then, mainly as a result of IR-observations of stars near Sgr A*.

The compact central radio source, Sgr A*, was first identified by Balick & Brown (1974), using the NRAO radio interferometer at Green Bank. It was later found by Brown et al. (1981) to be located close to the dynamical centre of the Galaxy, by observations with the VLA. The central radio source Sgr A* was shown to have variable activity (e.g. Brown & Lo 1982), both on short and long timescales. Eckart et al. (1993) showed that the centre of the NIR stars coincides with Sgr A* within fractions of an arcsecond. Near-infrared speckle imaging methods have created a set of proper motion data for the stars close to Sgr A* and traced trajectories down to a scale of only 5 light days, $\sim 1.3 \cdot 10^{16}$ cm, from the centre. The suggested mass enclosed within the inner 0.015 pc is $2.61 \pm 0.35 \cdot 10^6$ $M_\odot$ (Eckart & Genzel 1996, 1997; Ghez et al.1998). The characteristic size of such a mass is the Schwarzschild radius $r_s \equiv 2GM/c^2$, which is equal to $7.7 \cdot 10^{11}$ cm, or about 6.4 μarcsec, and an event horizon at about 35 μarcsec at a distance of 8 kpc. Stellar orbit investigations by Schödel et al. (2002) indicate an even higher central point mass of $(3.7 \pm 1.5) \cdot 10^6$ $M_\odot$ based on the observed stars pericentre distance of only 17 light hours from Sgr A*.

Ghez et al. (1998) found, based on stellar proper motions, that the gravitational potential peaks on Sgr A* within ~ 0.1 arcsecond, and Ghez et al. (2000) announced the first detection of acceleration in the motion of stars allowing calculation of their orbits and indicate that the dynamical centre of these trajectories coincides with Sgr A* to within 50 mas.

The accuracy of the position and proper motion of the central source have been estimated by Menten et.al (1997), Eckart et.al (1993), Ghez et.al (1998, 2000). The upper limit of the size of Sgr A* from proper motion measurements is found to be about 1 μarcsec and the lower limit about 0.1 μarcsec, i.e. between 10^{11} and 10^{10} cm. To demonstrate that Sgr A* is not star-like Rogers et al. (1994) and Krichbaum et al. (1998) demonstrate that it is compact on a scale at or below 0.1 mas ($1.3 \cdot 10^{13}$) cm for the highest frequencies, corresponding to ~ 17 Schwarzschild radii for a $2.6 \cdot 10^6$ $M_\odot$ black hole. The limit of the size indicates brightness temperatures between ~ 10^{10} and 10^{12} K, which is in the regime of a typical Active Galactic Nucleus, AGN (Readhead 1994). Based on present state of knowledge it is reasonable to assume that the true dynamical centre of the Galaxy is a massive black-hole at the position of Sgr A*.

The spectrum of the central parsec consists of free-free emission, dust emission, optical/UV emission and soft X-ray emission. The Sgr A* radio spectrum resembles that of a weak Seyfert 1 nucleus of a few 10^8 $L_\odot$ (Mezger et al. 1996) since it is brightest at UV and X-ray wavelengths, shows broad emission lines, e.g. Hα, Hβ, NII and varies in brightness by up to 50% in a few months. In general it can be explained by synchrotron emission from quasi-monoenergetic relativistic electrons (Duschl & Lesch 1994). The radiation from Sgr A* is circularly polarized (Bower et al. 1999) and is variable on a timescale of 10 days in the GHz frequency band (Bower 2000). The size of Sgr A* in the radio regime is $\leq 2.5 - 4 \cdot 10^{13}$ cm, and its flux density is ~ 9 mJy, in its dereddened K-band. The luminosity is $\leq 10^3$ $L_\odot$ if black-body radiation from an object with a single temperature of about $4 \cdot 10^4$ K is assumed. The X-ray luminosity is less than a few 10^2 $L_\odot$. With the mass and luminosity for Sgr A* the accretion rate appears to be about five orders of magnitude too low. Sgr A* is therefore heavily under-luminous, and the best candidate for the Sgr A* is a "starving" black hole.

There is, however, no observational evidence for the presence of a Standard Accretion Disk which would be expected surrounding a black hole. On the other hand, Morris reports, at the Galactic Centre Conference 2002, a pair of bipolar X-ray lobes, perpendicular to the Galactic plane and roughly symmetrical about Sgr A*, observed with the ACIS-Instrument on the Chandra X-ray Observatory. The lobes have a gas density of ~ 1 cm^{-3}, are about 15 pc long and show an outflow velocity of about 1000 kms^{-1}, which would indicate a time scale of ~ 10^4 yr.

The central radio source, Sgr A*, currently accepts only a fraction of the infalling material. Recent observations support the idea of a mass inflow rate varying with time. The inflow could temporarily be halted by mass-outflow winds from IR-stars in the central parsec. The concept of recurrent phenomena in Sgr A* is now generally accepted, and time scales of the order of days have been observed and variations of some hundred thousand years have been anticipated. The explanation of recurrence is, however, not yet understood – suggested candidates are the existence of a precessing black hole or a double rotating black hole at the GC, as reported by Liu and Scoville respectively, at the Galactic Centre Conference 2002.

3.8. Relative positions of features at the Galactic Centre

When interpreting spectral line data, one should keep in mind that the combination of two-dimensional projected positions with radial velocity as a third dimension does not contain sufficient information to allow for a unique deprojection into three dimensional space. Such a determination of the third spatial coordinate always carries the risk of misinterpreting a coincidence of features that are projected onto the same position in two-dimensional space and which by chance exhibit similar radial velocities without being physically connected. This necessarily introduces a certain ambiguity in the subsequent interpretation. By the use of deductive methods, i.e. combination of independent observations, observation of velocity gradients, mass estimates, observation of symmetric phenomena, etc. and fitting of theoretical models it is possible to rule out some of the ambiguities concerning the location of objects.

The relatively large velocity gradient of ~ 4 kms^{-1} /pc, assuming R = 8 kpc, in the Molecular Belt connecting the centres of the +20 kms^{-1} cloud and the +50 kms^{-1} cloud is consistent with a location in the central 20 parsec of the Galaxy. However, several interpretations exist of the relative positions, kinematics and interrelation of the features of the Sgr A Cloud Complex, e.g. Sandqvist (1974, 1989), Genzel et al. (1989, 1990) and Coil & Ho (2000). Zylka (1996) supports the idea that the +20 kms^{-1} and +50 kms^{-1} clouds are in fact one coherent structure, and Poglitsch et al. (1991) that there is a physical connection between the GMCs and the central few parsec of the GC.

A result of this thesis is that the +50 kms^{-1} and +20 kms^{-1} molecular clouds are condensations in the continuous Molecular Belt, and that the dominant absorption moves westward as the velocity decreases. Furthermore, it is concluded that a part of the Molecular Belt is possibly located behind Sgr A West and in front of Sgr A East. No absorption against the Molecular Belt is seen towards the compact HII regions, which may indicate that these star forming sites lie on the near side of the Molecular Belt and possibly on the near side of the +50 kms^{-1} molecular cloud. An extended discussion of the relative positions of the Molecular Belt, Sgr A East, Sgr A West and Sgr A* is found in Karlsson et al. (2003 Paper III, 2003 Paper IV).

Chapter 4

The Hydroxyl Radical – OH

4.1. Why study OH?

The OH molecule is easy to detect at 6 and 18 cm, both in emission and absorption, and the abundance of OH is relatively high in the GC. OH is also associated with other observable atoms, molecules and ions such as OI, CO, H_2O, HCN, HCO^+, HNO_3, NH_3, H_3O^+, etc. Some important chemical reactions of OH are shown in Fig.15 (Avrett 1979). The different species could be used as first order tracers of volume densities, e.g. HCN ~ 10^5 cm^{-3} and CO ~ 10^3 cm^{-3}.

OH was first discovered in absorption in 1963 and in emission in 1965. Observation of the OH absorption lines serves as a tool to map the kinematics of the molecular clouds and a means to determine their densities and masses. Furthermore, the relative intensities of the OH transition lines may give information of the physical environment, at least its limits. The first interferometry measurement of OH masers was made in 1966 by Rogers et al. and Davies et al., and in the same year the theory of cosmic masers was developed.

Many absorption line and point-source observations of OH in the GC have been published, e.g. Robinson & Mc Gee (1970), Sandqvist (1974), Bieging (1976), Lindqvist et al. (1992), Boyce & Cohen, (1994), Sjouwerman et al. (1998). The investigation presented in this thesis is the first both high angular and high velocity resolution observation of all four OH emission and absorption transition lines at 18 cm.

4.2. OH chemistry

In a diffuse cloud, H_2O is dissociated on a timescale of about 30 years in the obscured interstellar radiation field by ultraviolet photons,

$$H_2O + h\nu \rightarrow OH + H, \qquad (4\text{-}1)$$

The OH radicals may be destroyed by direct photodissociation by the reaction,

$$OH + h\nu \rightarrow O + H, \qquad (4\text{-}2)$$

and by the chemical reactions

$$OH + C^+ \rightarrow CO^+ + H \qquad (4\text{-}3)$$

$$OH + C^+ \rightarrow CO^+ + H^+ \qquad (4\text{-}4)$$

The mean time for photodissociation is about 300 years in the unshielded radiation field but increases exponentially with depth into the cloud as the grains absorb the dissociating

photons. For a cloud of density 100 cm^{-3} with a C^+ abundance of 10^{-2}, the chemical and photodissociation times are comparable at the edge of the cloud but shorter in the interior. Thus chemical reactions determine the destruction of OH throughout most of the cloud.

The reaction (4-3) is often followed by the rapid reaction

$$CO^+ + H_2 \rightarrow HCO^+ + H \qquad (4\text{-}5)$$

But in clouds where the $n(H)$ is comparable to $n(H_2)$ the reaction:

$$CO^+ + H \rightarrow CO + H^+ \qquad (4\text{-}6)$$

also occurs. Both reactions (4-4) and (4-6) produce H^+, which acts as a catalyst for the formation of OH and H_2O.

As seen from above the presence of OH may be indicative of other molecules in the reaction chain and vice versa, and observations of the different species are often complementary, e.g. as shown in the chemical reactions (4-1) to (4-6) (Avrett 1979).

H^+ does not react with H or H_2, and cannot undergo dissociative recombination. It can be removed by slow radiative recombination, which is the dominating process in HII regions.

$$H^+ + e \rightarrow H' + h\nu \qquad (4\text{-}7)$$

where the prime indicates an excited state. The H^+ ion may transfer charge with O to form O^+, since the ionization potentials of atomic hydrogen and oxygen are nearly identical:

$$H^+ + O \rightarrow H + O^+ \qquad (4\text{-}8)$$

In the absence of any molecules the O^+ ions undergo radiative recombination, and its reversed reaction;

$$O^+ + e \rightarrow O + h\nu \qquad (4\text{-}9)$$

$$O^+ + H \rightarrow O + H^+ \qquad (4\text{-}10)$$

In the presence of only small amounts of molecular hydrogen the O^+ ions react rapidly with H_2 in the hydrogen abstraction reaction

$$O^+ + H_2 \rightarrow OH^+ + H \qquad (4\text{-}11)$$

Followed by the rapid reactions:

$$OH^+ + H_2 \rightarrow H_2O^+ + H \qquad (4\text{-}12)$$

$$H_2O^+ + H_2 \rightarrow H_3O^+ + H \qquad (4\text{-}13)$$

The H_3O^+ ion is chemically saturated and does not react further with H_2, and is removed by dissociative recombination and forming H_2O, OH, and atomic and molecular H:

$$H_3O^+ + e \rightarrow H_2O + H \quad (4\text{-}14)$$

$$H_3O^+ + e \rightarrow OH + H_2 \quad (4\text{-}15)$$

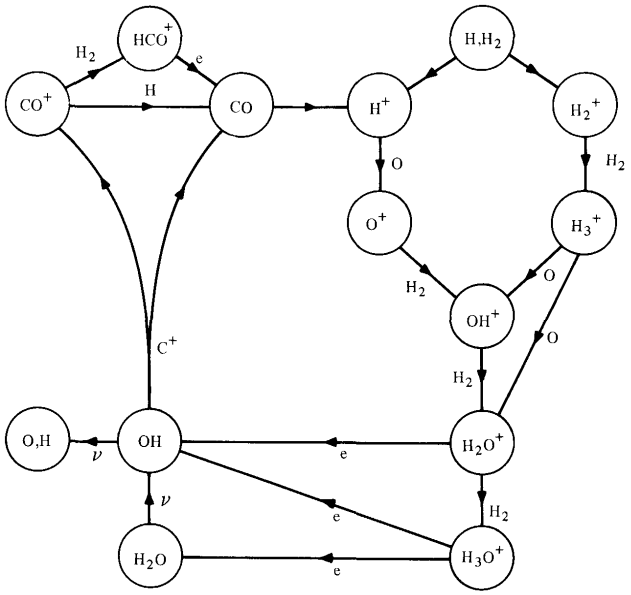

Fig. 15. The H^+, OH, HCO^+, and CO chemistry in an H_2 cloud (Avrett 1979).

4.3. Lambda-type doubling of the OH-transition lines

The OH molecule has a complicated spectrum, although it has an apparently simple physical structure. It depends on the facts that the ground state is: $^2\Pi$, ($\Lambda = 1$, $S = ½$), which leads to significant interactions among the spin and orbital angular momenta of the electrons and the rotational angular momentum, and that the OH molecule is light and rotates fast. The OH molecule is a radical, i.e. it is extremely chemically active and has a short lifetime in a terrestrial environment. The physics of the OH molecule at the densities and temperatures prevailing in the vicinity of the GC relies on a theoretical basis and upon computer simulations, since relevant laboratory experiments cannot be performed with present technology.

The OH-molecule possesses an electric dipole-moment, and the molecular transition lines involve electric dipole transitions which are much more intense than the magnetic dipole transitions of, for example, the hydrogen molecule. The OH-transition probability is also higher, $A_{10}{}^{OH} = 7.71 \cdot 10^{-11}\ s^{-1}$ vs. $A_{20}{}^{H_2} = 2.95 \cdot 10^{-11}\ s^{-1}$. As a result, it is possible to detect the OH lines even where the OH abundance is much less than that of hydrogen. The OH energy transitions at the temperatures and densities in the Galactic Centre are considered as pure rotational and no vibrationally excited lines have been detected.

The OH-molecule has two fine-structure levels in the $^2\Pi$ ground state, $^2\Pi_{1/2}$ and $^2\Pi_{3/2}$. The $^2\Pi_{3/2}$ state has the lower energy and is the only significant energy level at interstellar temperatures. The interaction of the electron angular momentum and the rotational angular momentum splits each level into two – the lambda doubling – giving rise to the main transition lines at 1665 and 1667 MHz of the $^2\Pi_{3/2}$ state. The lambda populations are very sensitive to the surrounding physical parameters. The OH molecule also shows a net nuclear spin of ½, and interaction with the hydrogen nucleus causes hyperfine-splitting of the two lambda doublet lines (Fig.16), creating the satellite lines at 1612 and 1720 MHz. The hyperfine lines of the $^2\Pi_{3/2}$ state may also be subject to Zeeman-splitting in the presence of a magnetic field.

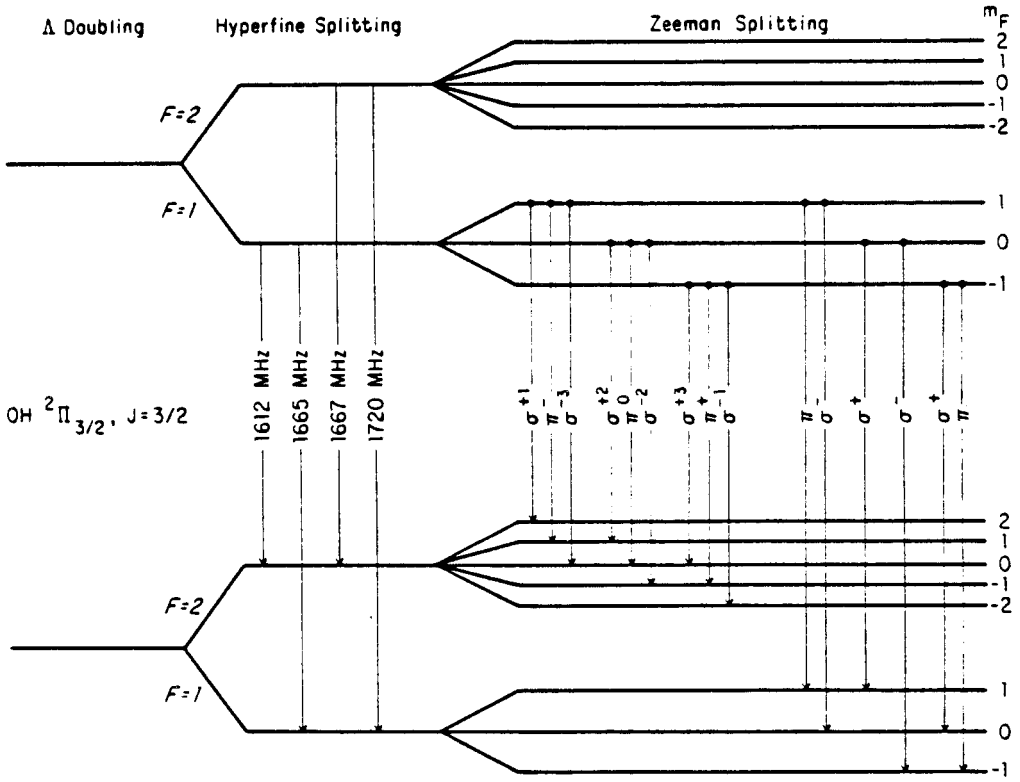

Fig. 16. Energy levels of the OH molecule in its ground state. The permitted Zeeman transitions at 1612 and 1665 MHz are indicated (Winnberg 1984).

The four 18-cm spectral lines at 1612, 1665, 1667 and 1720 MHz that are seen in emission and absorption are the result of rotational energy transitions of the OH molecule. For thermodynamic equilibrium and a weakly absorbing medium, the line intensities are related as: 1: 5: 9: 1. In case of a strongly absorbing medium the line ratios should, however, approach unity due to saturation effects. OH is very sensitive to the surrounding radiation field and the energy populations are often deviating from thermodynamic equilibrium leading to masering effects. OH is masering at all four transitions, especially strong at 1612 and 1720 MHz. The 1612-, 1665- and 1667-MHz OH masers trace star formation regions and shocks, while the 1720-MHz masers are associated with supernova remnants, see Chapter 3.

4.4. Absorption lines of the OH molecule

It is assumed that the background continuum radio source related to in this work is the integrated emission of the Galactic background and the discrete radio sources in the GC. The continuum radiation is composed of synchrotron emission, free-free and free-bound transitions from thermal electrons.

The radiation from the background is partially absorbed while passing through the molecular gas of brightness temperature T_S, and the observed brightness temperature T_b *(v)* at the frequency *(v),* for a homogenous medium is given by equation 4-16, which is the "radio-solution" of the general equation of radiative transfer:

$$T_b(v) = T_S\,(1 - e^{-\tau(v)}) + T_C\, e^{-\tau(v)} \qquad (4\text{-}16)$$

where the first term represents the emission from the gas cloud and the second term is the attenuated radiation from the background, whose brightness temperature is T_C, which is considered constant over the frequency interval occupied by the line. $\tau(v)$ is the optical depth related to the absorption coefficient and the path length in the gas. It is assumed that the Rayleigh Jeans relation can be used, since $hv << kT$.

In spectral line observations, we are generally interested in the difference between the brightness temperature at the line frequency $T_b(v)$, and the brightness temperature outside the line, T_C, i.e. the brightness temperature T_L of the spectral line.

$$T_L = T_b(v) - T_{C,} \qquad (4\text{-}17)$$

$$= (T_S - T_C)(1 - e^{-\tau(v)}) \qquad (4\text{-}18)$$

If $T_S > T_C$ the line appears in emission and if $T_S < T_C$ the line is seen in absorption.

Determination of $\tau(v)$ requires a model of the background continuum along the line of sight. The different continuum sources have to be separated and related to the respective absorption feature to determine the optical depth and for subsequent determinations of column density and mass of the observed feature. This process is postponed to a coming paper.

In the present work we have assumed that the entire continuum is behind the OH gas and that the emission is zero in the absorbing clouds. Maps of the line-to-continuum ratio have been produced. If, as in our absorption case, the line temperatures T_L are negative (see Eq. 4-18), it is in fact the $-T_L/T_C$ values that we calculate. The $-T_L/T_C$ maps are subsequently used as indicators of the variation of the OH column density.

The line profiles of the OH molecule at 18 cm observed towards Sgr A with an angular resolution of 18 arcmin are shown in Figs. 17 and 18 (Sandqvist 1973). Note that the profiles of 1665 and 1667 MHz overlap. Several absorption features can be identified in the profiles, e.g. +20 and +50 kms^{-1} clouds, the EMR at –130 kms^{-1}, the 3-kpc arm at –50 kms^{-1} and the local Sagittarius Arm at 0 kms^{-1}.

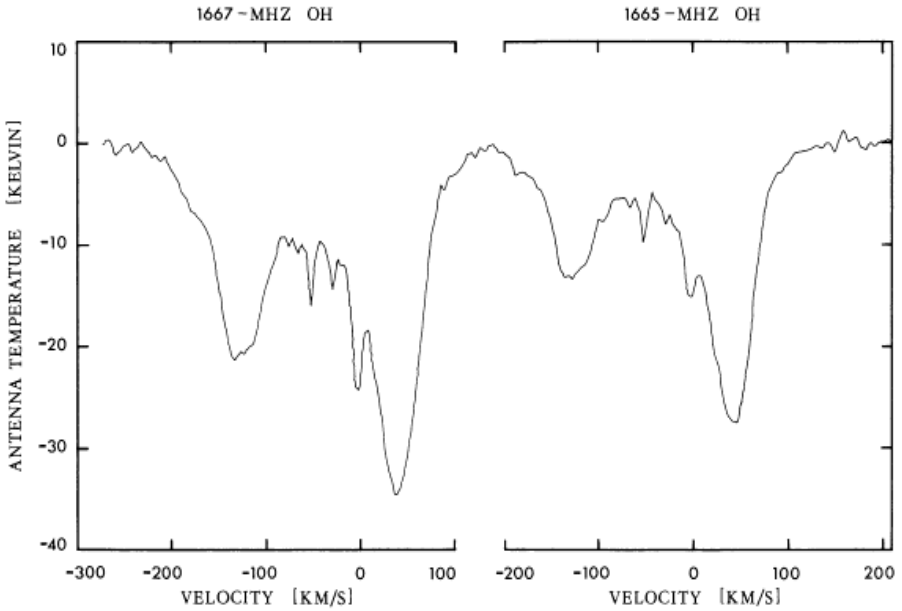

Fig. 17. The 1667- and 1665-MHz OH main line profiles observed towards Sgr A with a resolution of 18 arcmin (Sandqvist 1973).

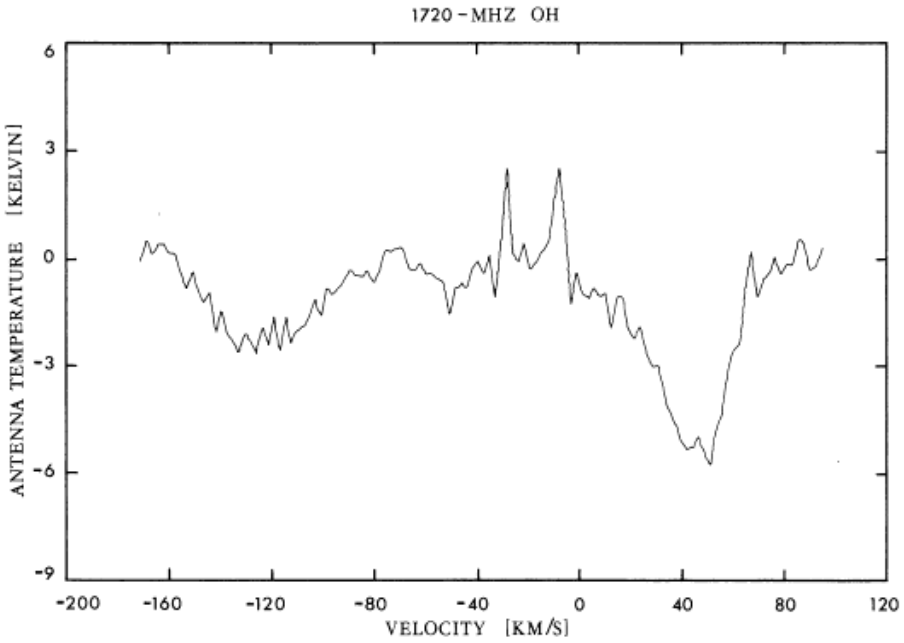

Fig. 18. The 1720-MHz OH satellite line profile observed towards Sgr A with a resolution of 18 arcmin (Sandqvist 1973).

Chapter 5

Observations and Data Reduction

5.1. Observations

Observations of the two 1665- and 1667-MHz OH main lines, and the two 1612- and 1720-MHz satellite lines at 18 cm were made with the VLA in its (extended) BnA configuration. The two main lines were also observed with the (compact) DnC configuration. A summary of the observations is shown in Table 1.

Frequency (MHz)	HPBW ("x")	PA (°)	Resolution (kms^{-1})	$t_{integration}$ (minutes)
BnA configuration, 18 antennas, R-pol. June 1986				
1612	4.0 x 2.7	55.7	9.1	144
1665	3.9 x 2.9	64.7	8.8	169
1667	4.0 x 2.8	61.1	8.8	173
1720	3.7 x 2.7	57.1	8.5	148
DnC configuration, 27 antennas, R and L-pol. October 1989				
1665	24.0 x 22.3	29.8	8.9	144
1667	30.2 x 23.7	46.3	8.8	136

Table 1. Observations summary.

5.2. Data reduction

Following absolute calibration and calibration for known instrumental effects according to VLA standard procedures, the data were further processed to produce velocity channel images. All data processing was performed in the NRAO Astronomical Image Processing System, AIPS, except for the images in Paper I, which were produced by "Bildprogram för Finsmakare BIFF" (Högbom ~ 1985).

The data for Papers I and II, the BnA-array 1667-MHz observations, were reduced in the mid-eighties with the contemporary computer technology. Due to limited processor speeds and memory size, it was then not possible to produce and process large image cubes, so the maps were produced individually and stored on tape. Consequently, reducing the data was very time consuming compared to the processing time for Papers III and IV. Further, the map size

in the earlier sessions was limited to 128 x 128 pixels, except for the continuum map which was made 256 x 256 pixels, while the later maps were made 512 x 512 or 1024 x 1024 pixels.

5.3. Map production

Papers I and II

A continuum map was constructed by selecting three line-free channels on each side of the 1667-MHz line, and taking the average. The resulting map was CLEANed (Högbom 1974) and used as continuum map for subtraction from the velocity channel maps. The continuum map is shown in Paper I, Fig. 2. After subtracting the continuum, the velocity line maps were also CLEANed. In some areas and at certain velocities, weak extended emission at about 3σ remained in the maps. The nature of the emission was much debated and four possible explanations were suggested: a) an imperfect continuum map was used in the subtraction, i.e. containing some residual absorption line, b) an artefact resulting from instabilities in the CLEAN algorithm triggered by noise (Cornwell 1982), c) lack of zero- and short-spacing observations causing a "bowl" in the centre of the maps, and d) a real feature.

Much effort was paid to the quality of the continuum map. The number of line-free velocity channel maps was varied between 1 and 8, on one and both sides of the line, and averaged into continuum maps, which consecutively were subtracted from the data set. However, the extended emission remained almost unchanged. The number of CLEAN iterations and depth of cleaning were also varied in wide ranges with no significant effect on the extended emission features.

As a result, the effects of a) and b) were ruled out, but we were not able at this stage to conclude about the alternatives c) and d).

Papers III, IV and Appendix

Recently, all four lines of the BnA observations and both lines of the DnC observations have been processed with the current state-of-art computers and again, the AIPS software. Map cubes of the lines with full angular coverage were produced, processed and stored on disk for easy access and further image processing.

The 1665- and 1667-MHz continuum map was made in the image plane using the AIPS task IMLIN, which produces a continuum by a linear fit over the featureless channels of each side of the combined 1665- and 1667 MHz image cube. The resulting IMLIN continuum image was used for self-calibration of the phases in the data set. Maps were made with 1024 x 1024 pixels of 0.75" with both the CLEAN and the maximum entropy algorithm MEM (AIPS VTESS). There were no significant differences in the maps produced by the two methods, but the maximum entropy method was faster and the noise was somewhat reduced.

Extended emission was still present both in the BnA and DnC maps. In particular, clear extended emission features were observed in the DnC maps at certain velocities, see further details in Chapter 6.

For the 1612- and 1720-MHz lines the AIPS task UVLIN was used to subtract a linear fit over frequency to the continuum directly in the *u,v* plane. A strong maser spot was used to self-

calibrate both phases and amplitudes and 1024 x 1024 pixel maps were produced. The 1612- and 1720-MHz maps were processed by CLEAN, while the 1665- and 1667-MHz maps were enhanced by the MEM algorithm. The 1612- and 1720-MHz maps were also checked for consistency by the MEM, but no significant differences were found.

$-T_L/T_C$ maps for certain velocities of the OH-Streamer and the HNVG were also produced to verify the validity of these features versus the continuum background.

Chapter 6

Results

The two sets of BnA and DnC data comprise altogether about 350 velocity channel maps. This thesis mainly discusses the BnA configuration observations. A summary of the results is presented below, while a more detailed analysis and discussion of the results is provided in Papers I – IV.

Furthermore, a set of absorption line maps of the 1665- and 1667-MHz DnC observations is presented in the Appendix, and some brief results of the DnC array data are presented in Sect. 6.2.

6.1. VLA BnA OH observations at 1612, 1665, 1667 and 1720 MHz

Perhaps the most intriguing result is the discovery of the OH-Streamer presented already at the Townes Symposium in 1986 (Paper I), although it was called the "sweeper" at that time. The OH-Streamer is observed at all frequencies, except for the 1720-MHz line. The $-T_L/T_C$ maps in Paper III and IV provide further evidence of the reality of this feature. The interpretation of its geometric relationship with the CND and Sgr A* is however not fully understood and is suffering from the lack of a mass determination and an orbital model of the OH-Streamer. This problem will be addressed in a coming paper.

6.1.1. OH absorption, main observational results

a) A new OH-Streamer inside the CND at velocities between ~ +76 and –20 kms^{-1}, is observed at 1612, 1665 and 1667 MHz and seems, in projection, to stretch from the southwestern part of the CND, through the empty Central Cavity and eventually ending up at Sgr A*.

b) OH absorption is observed from the CND northeastern and southwestern components with peaks at about +100 and –80 kms^{-1}, respectively.

c) Strong OH absorption is seen towards most of the eastern and western parts of the Sgr A East shell.

d) A general lack of OH absorption is detected towards Sgr A West at velocities of the Molecular Belt.

e) OH absorption is observed against SgrA West North Arm at ~ +6 kms^{-1}.

f) OH absorption of the Molecular Belt +50 kms^{-1} cloud is seen against the Sgr A East structure.

g) Lack of absorption against the compact HII regions at velocities of the Molecular Belt.

h) OH absorption of the Molecular Belt +20 kms^{-1} cloud is seen against the Sgr A East structure.

i) OH absorption is observed against Sgr A* at +43 to –36 kms^{-1} and –142 to –151 kms^{-1}, but not at velocities of the Molecular Belt.

j) A double-lobed structure of the HNVG is observed to the northeast and southwest[1] of Sgr A*, most prominent at about –170 kms^{-1}.

k) OH absorption of the EMR is seen at –126 to –143 kms^{-1}.

l) Weak absorption is detected against the compact HII regions at –126 kms^{-1}, i.e. at the velocities of the EMR.

6.1.2. Point-like OH emission, masers

a) 45 new OH masers were found at all four 18-cm OH transition lines, 10 of which are new discoveries.

b) A new maser was discovered in the CND at –132 kms^{-1} as a symmetric counterpart to a known maser at +132 kms^{-1}, which enabled the determination of the enclosed mass, see Sect. 3.3.

[1] In Paper III, caption of Figure 3, the direction of the double-lobed structure should read “northeast to southwest”.

6.1.3. Extended OH emission

Weak extended diffuse emission was observed in some of the main line maps, e.g. Fig. 8 in Paper IV. The origin of that emission is discussed in Paper IV, but no final conclusion about the origin was made at that time, see also Sect. 5.3. Indeed, there are observations of weak extended OH emission in the Galactic Centre in the 1720-MHz line (e.g.Yusef-Zadeh et al. 1999), and in other galaxies at 1667 MHz (Pihlström et al. 2001), but it is also known that the lack of zero- and short-spacing information in interferometer observations may give spurious effects in the images. It seemed that a deep analysis was warranted, and the next step would be to concatenate the BnA and DnC observations to reduce the unfilled areas in the *u*,*v* plane. Recently, this has been done and is reported briefly in Sect. 6.3.

6.2. VLA DnC observations at 1665 and 1667 MHz

A set of 96 velocity channel maps of the OH absorption observed at 1665 and 1667 MHz with the DnC array are provided in the Appendix. Included are also maxmaps and minmaps for the same area which includes the Sgr A Complex, the Bridge and the Arc. The maxmap/minmap presentation method was developed by Sjouwerman (1997). The maxmaps/minmaps are produced through projection of the three-dimensional data cube onto a two-dimensional sky image map, i.e. by storing the maximum or minimum intensity over the whole velocity axis for each pixel in the sky plane. The maxmaps are useful tools for identifying point-like maser sources and possible regions of extended emission, while the minmaps give an overall view of the spatial distribution of the absorption.

6.2.1. OH absorption features, preliminary results

- The HNVG is seen in OH absorption at 1665 and 1667 MHz. The HNVG can be traced out to –231.7 kms^{-1}.

- The northwestern protrusion of the Sgr A halo can be seen in absorption from –196.5 to –29.2 kms^{-1}.

- The Expanding Molecular Ring can be followed in absorption across Sgr A, the thermal "Bridge" and the non- thermal "Arc" from velocities of –152.5 kms^{-1} and towards less negative velocities.

- Absorption towards the "Pistol" and "Sickle" region in the Arc can be traced between –117.2 and –46.8 kms^{-1}.

- An OH absorption region extends southwards from the Sgr A continuum halo in maps at velocities of –29.2 to +23.6 kms^{-1}.

- The Molecular Belt and its associated velocity gradient are present at least in the +14.8 to +67.7 kms^{-1} maps.

- The northeastern part of the CND is traced clearly from +94.1 to +164.5 kms^{-1} in the velocity maps of the 1665-MHz OH absorption line.

6.2.2. Emission features

Clear extended emission features at about 6σ level were observed in some individual 1667-MHz velocity line maps. For example, between +41.2 to +67.7 kms^{-1} (Fig. 20), where emission is seen in an area ~ 4′ x 3′ wide, in the northwestern part of the Sgr A halo. The reality of the tantalizing emission features was questioned, keeping in mind the wise words about the VLA by Ekers (1982): "The problem is that if you find a new and unexpected effect in your observation it is most likely to be an instrumental error."

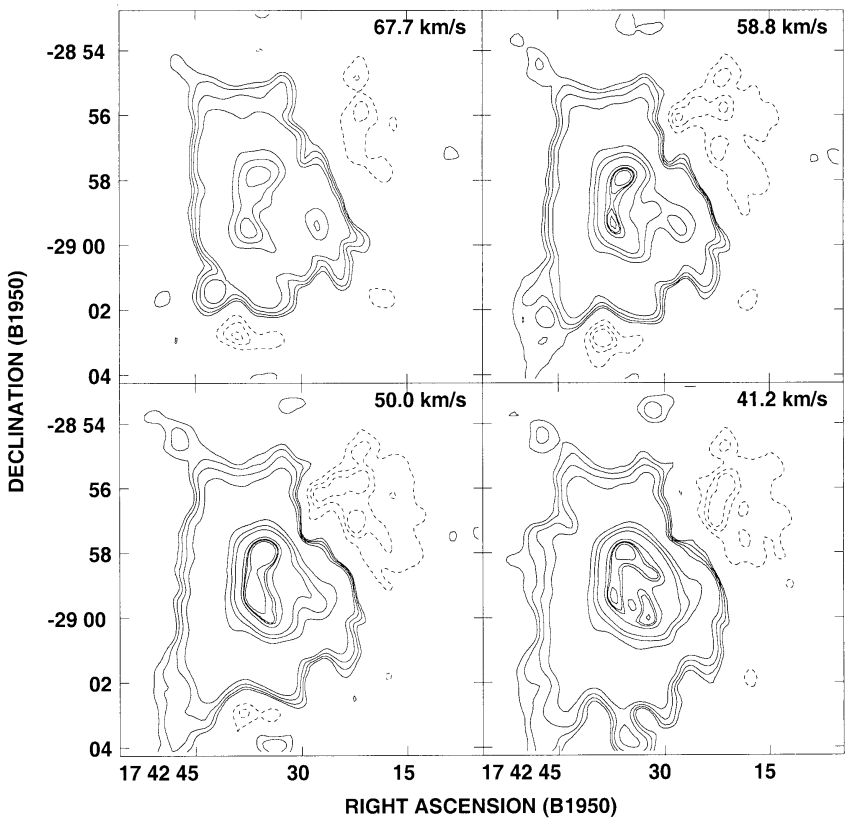

Fig. 20. 1667-MHz OH absorption and emission (DnC-array) for four selected velocities, shown in upper right corners. The extended emission feature is seen to the northwest of the Sgr A Complex. Absorption contours (solid lines) are at 50, 70, 100, 150, 1000, 1500, 2000, 3100, 3400, 3500 and 3700 mJy; emission contours (dashed lines) are at 50, 80, and 100 mJy.

6.3. Concatenation of BnA and DnC observations

Interferometers are inherently limited by the shortest sampling baseline. The uncovered area represents a "hole" in the centre of the *u,v* plane resulting in loss of the large-scale flux. To measure the true flux, single-dish observations are required. If, however, data from observations with different baseline configurations are combined it is possible to recover some of the missing flux. The combination, or concatenation, of the data can be made during or after deconvolution, or preferably prior to imaging by procedures and techniques in AIPS.

By the courtesy of Miller Goss at NRAO, the BnA and DnC observations have recently been concatenated. A quick look at those data revealed that the emission features seen in Fig. 20,

were not reproduced in the concatenated data base. Our preliminary conclusion is that the extended emission features in the absorption maps were an instrumental artefact. However, this result requires further study and interpretation.

At this point, two images based on the concatenated data have been produced and are shown in Figs. 8 and 21. In Fig. 21, showing the continuum emission, both the large scale structures of the Sgr A Complex the Arc and the Bridge are seen, as well as the smaller-scale features: the Sgr A East shell, Sgr A West and Sgr A*.

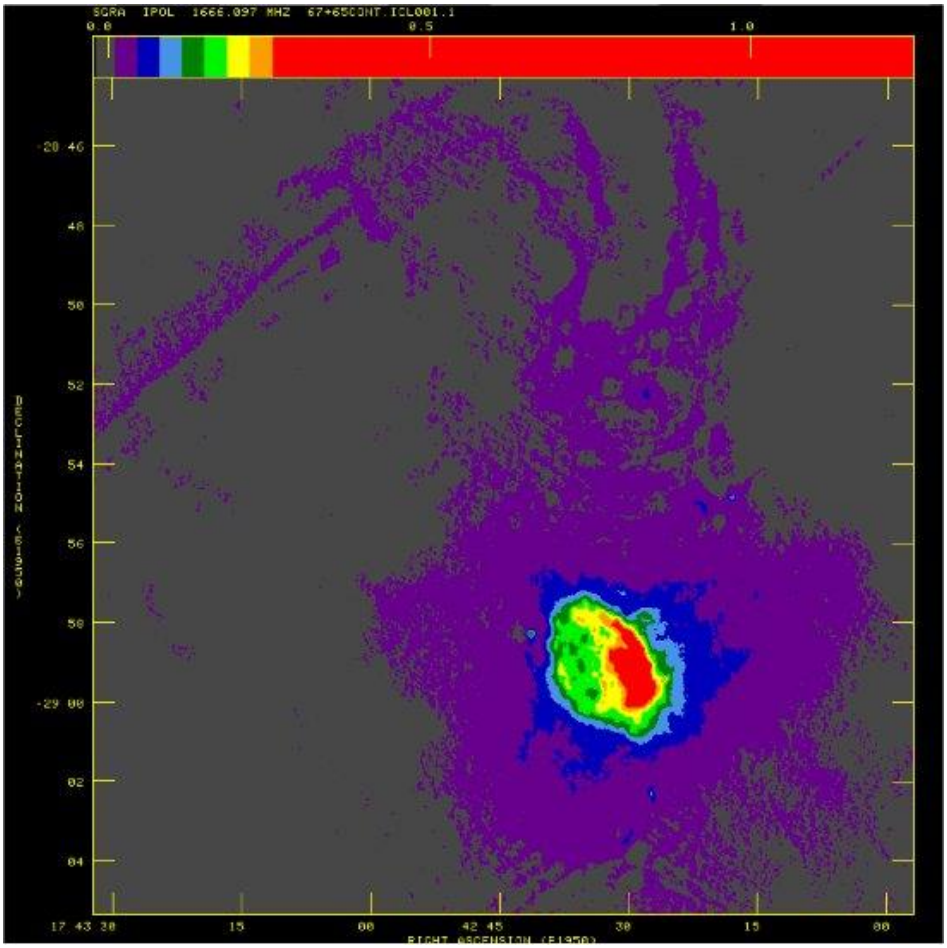

Fig. 21. The Sgr A Complex, including the Arc, the Bridge, the Halo, the Sgr A East shell, Sgr A West and Sgr A*, are seen in this 18-cm radio continuum image of the concatenated BnA and DnC data, observed in 1986 and 1989 (Karlsson et al. 2004, in preparation).

Chapter 7

Future outlook

The forthcoming analysis of the observations will primarily be based on the concatenated BnA and DnC data set. Below is a tentative list of interesting areas for an extended and deeper analysis of the existing data:

- determine the physical parameters of the observed features, i.e. density, mass and linear dimensions from the present observations.

- develop an orbital model of the OH-Streamer given its mass distribution and velocity field from these observations.

- develop a model of the relative location of the observed features in the GC.

- perform a deep search for new features in the concatenated data base and conduct a comparative study with observations of other species.

- study the observed maser sources in relation to star formation sites and large-scale shock waves.

Acknowledgements

I am very grateful to my supervisor, Professor Aage Sandqvist, for keeping trust and spirit even during the idling periods of this work. I am also grateful to Dr Lorant Sjouwerman for help with processing of maps and for the contribution about masers, and to Assoc. Professor Jan Högbom for introducing me to the world of interferometers, image processing, etc. I also thank Professors Per Olof Lindblad and René Liseau for reading the manuscript and supplying me with comments and constructive criticism in the process of preparing the thesis. This research was supported by the Swedish Research Council. I also acknowledge the open policy for the use of NRAO's VLA. The National Radio Astronomy Observatory (NRAO) is operated by National Science Foundation.

References

Aitken D.K., Smith C.H., Roche P.F., Wright C.M. 1990, MNRAS 246, 1
Armstrong J.T., Barrett A.H. 1985, ApJS, 57, 535
Avrett E.H. 1979, ed. Frontiers of Astrophysics
Balick B., Brown R.L. 1974, ApJ 194, 265
Begelman M.C., Frank J., Shlosman I., 1989, Theory of Accretion Disks, eds. F. Meyer, W.J. Duschl, J. Frank, E. Meyer-Hofmeister, Proceedings of a NATO Advanced Research Workshop, held in Garching, Dordrecht: Kluwer 290, 373
Bieging J.H. 1976, A&A 51, 289
Binney J., Gerhard O.E., Stark A.A., Bally J., Uchida K.I. 1991, MNRAS 252, 210B
Bower G.C., Falcke H., Backer D.C. 1999, 195th AAS Meeting, Bulletin of the American Astronomical Society 31, 1463
Bower G.C. 2000, GCNEWS 11, 4, eds. Cotera A., Falcke H., Markoff S.
Boyce P.J., Cohen R.J. 1994, A&AS 107, 563
Brown R.L., Johnston K.J., Lo K.Y. 1981, ApJ 250, 155
Brown R.L., Lo K.Y. 1982, ApJ 253, 108
Coil A.L., Ho P.T.P. 2000, ApJ 533, 245
Coker R., Melia F. 1997, ApJ 488, 149
Cornwell T. 1982, NRAO/VLA WORKSHOP: SYNTHESIS MAPPING, 9
Duschl W. J., Lesch H. 1994, A&A 286, 431
Eckart A., Genzel R., Hofmann R., Sams B.J., Tacconi-Garman L.E. 1993, ApJ 407, 77
Eckart A., Genzel R. 1996, Nature 383, 415
Eckart A., Genzel R. 1997, MNRAS 284, 576
Ekers, R.D. 1982, Synthesis Mapping, Proc of the NRAO-VLA Workshop Socorro, iv
Ekers R.D., van Gorkom J.H., Schwarz U.J., Goss W.M. 1983, A&A 122, 143
Frail D.A., Goss W.M., Slysh V.I., 1994, ApJ 424, L111
Gatley I., Beattie D.H., Lee T.J., Jones T.J., Hyland A.R. 1984, MNRAS 210, 565
Gatley I., Jones T.J., Hyland A.R., Wade R., Geballe T.R. 1986, MNRAS 222, 299
Geballe T.R., Krisciunas K., Lee T.J., Gatley I., Wade R., Duncan W.D., Garden R., Becklin E. E. 1984, ApJ 284, 118
Geballe T.R., Wade R., Krisciunas K., Gatley I., Bird M.C. 1987, ApJ 320, 562
Genzel R., Townes C.H. 1987, ARAA 25, 377
Genzel R., Stacey G.J., Harris A.I., Townes C.H., Geis N. 1989, IAU-Symp 136, 151
Genzel R., Stacey G.J., Harris A.I., Townes C.H., Geis N., Graf U.U., Poglitsch A., Stutzki J. 1990, ApJ 356, 160
Genzel R., Hollenbach D., Townes C.H. 1994, Rep. Prog. Phys. 57, 417
Genzel R., Thatte N., Krabbe A., Kroker H., Tacconi-Garman L.E. 1996, ApJ 472, 153
Gerhard O.E., Stark A.A., Bally J., Uchida K.I. 1991, MNRAS 252, 210
Ghez A.M., Klein B.L., Morris M., Becklin E.E. 1998, ApJ 509, 678
Ghez A.M., Morris M., Becklin E.E., Tanner A., Kremenek T. 2000, Nature 407, 349
Güsten R., Downes D. 1981, A&A 99, 27
Güsten R., Walmsley C.M., Pauls T. 1981, A&A 103, 197
Güsten R., Genzel R., Wright M.C.H., Jaffe D.T., Stutzki J., Harris A.I. 1987, ApJ 318, 124
Hall D.N.B., Kleinmann S.G., Scoville N.Z. 1982, ApJ 260, 53
Hauser M.G., Kelsall T., Leisawitz D., Weiland J. 1995, COBE DIRBE Explanatory Supplement Vers. 2.0, COBE Ref. Pub. No. 95-A (Greenbelt, MD: NASA/GSFC)

Hildebrand R.H., Gonatas D.P., Platt S.R., Wu X.D., Davidson J.A., Werner M.W., Novak G., Morris M. 1990, ApJ 362, 114
Högbom J. 1974, A&AS 15, 417
Högbom, ~ 1985, Bildprogram för Finsmakare, BIFF, Stockholms Observatorium
Hüttemeister S., Wilson T.L., Bania T.M., Martin-Píntado J. 1993 A&A 280, 255
Jackson J.M., Geis N., Genzel R., Harris A.I., Madden S., Poglitsch A., Stacey G.J., Townes C.H. 1993, ApJ 402, 173
Kaifu N., Kato T., Iguchi T. Nature 1972, 238, 105
Karlsson R., Sandqvist Aa., Sjouwerman L.O., Whiteoak J.B. 2003 Paper III, Astronomische Nachrichten/AN, Suppl. Issue 1/2003
Karlsson R., Sjouwerman L.O., Sandqvist Aa., Whiteoak J.B. 2003 Paper IV, A&A 403, 1011
Killeen N.E.B., Lo K.Y., Crutcher R.1992, ApJ 385, 585
Koyama K., Awaki H., Kunieda H., Takano S., Tawara Y. 1989, Nature 339, 603
Koyama K., Maeda Y. 1996, IAUS 169, 287
Krichbaum T.P., Graham D.A., Witzel A., Greve A., Wink J.E., Grewing M., Colomer F., de Vicente P., Gomez-Gonzalez J., Baudry A., Zensus J.A.1998, A&A 335, 106
Lacy J.H., Townes C.H., Geballe T.R., Hollenbach D.J. 1980, ApJ 241, 132
Lebofsky M.J., Rieke G.H., Deshpande M.R., Kemp J.C. 1982, ApJ 263, 672
Lindqvist M., Winnberg A., Habing H.J., Matthew H.E. 1992, A&AS 92, 43 (L-92)
Lo K.Y., Claussen M.J. 1983, Nature 306, 647
Lynden-Bell D., Rees M.J. 1971, MNRAS 152, 461
Marshall J., Lasenby A. 1994, in: The nuclei of normal galaxies – Lessons from the Galactic Center, eds. Genzel and Harris, 175
Melia F., Falcke H. 2001, Annu. Rev. Astron. Astrophys. 39, 309
Menten K.M., Reid M.J., Eckart A. 1997, ApJ 475, 111
Mezger P.G., Zylka R., Salter C.J., Wink J.E., Chini R., Kreysa E., Tuffs R. 1989, A&A 209, 337
Mezger P.G., Duschl W.J., Zylka R. 1996, A&A 7, 289
Morris M., Serabyn E. 1996, Annu. Rev. Astron. Astrophys. 34, 645
Palmer P., Goss W.M. 1996, GCNEWS - Galactic Center Newsletter, eds. A. Cotera & H. Falcke 2, 3
Piddington J.H., Minnett H.C. 1951, Aust. J. Sci. Res. A 4, 459
Pihlström Y.M., Conway J.E., Booth R.S., Diamond P.J., Polatidis A.G. 2001, A&A 377, 413
Poglitsch A., Stacey G.J., Geis N., Haggerty M., Jackson J., Rumitz M., Genzel R., Townes C.H. 1991, ApJ 374, 33
Predehl P., Trümper J. 1994, A&A 290, 29
Readhead A.C.S. 1994, ApJ 426, 51
Reid M. J. 1993, Annu. Rev. Astron. Astrophys. 31, 345
Roberts D.A., Yusef-Zadeh F., Goss W.M. 1966 ApJ 459, 627
Robinson D.A., McGee R.X. 1970, Austr. J. Phys. 23, 405
Rogers A.E.E., Doelman S., Wright M.C.H., Bower G.C., Geoffrey C., Backer D.C., Padin S., Philips J.A., Emerson D.T., Greenhill L., Moran J.M., Kellermann K.I. 1994 ApJ 434, 59
Sanders D.B., Scoville N.Z., Solomon P.M. 1985, ApJ 289, 373
Sandqvist Aa. 1971, Lunar Occultations of the Galactic Center Region in HI, OH and CH2O Lines, PhD Thesis (University of Maryland)
Sandqvist Aa. 1973, A&AS 9, 391
Sandqvist Aa. 1974, A&A 33, 413

Sandqvist Aa., Karlsson R., Whiteoak J.B., Gardner F.F. 1987, The 18-cm OH Distribution in the Galactic Center Torus, in AIP Conf. Proc. 155, The Galactic Center, ed. D.C. Backer (AIP, New York), 95
Sandqvist Aa. 1989, A&A 223, 293
Sandqvist Aa., Karlsson R., Whiteoak J.B. 1989, OH in the Environment of Sgr A, in IAU Symp 136, The Center of the Galaxy, ed. M. Morris (Kluwer, Dordrecht), 421
Schödel R., Ott T., Genzel R., Hofmann R., Lehnert M., Eckart A., Mouawad N., Alexander T., Reid M.J., Lenzen R., Hartung M., Lacombe F., Rouan D., Gendron E., Rousset G., Lagrange A.-M., Brandner W., Ageorges N., Lidman C., Moorwood A.F.M., Spyromilio J., Hubin N., Menten K.M. 2002, Nature 419, 694
Schwarz U.J., Bregman J.D., van Gorkom J.H. 1989, A&A 215, 33
Schwarz U.J., Lasenby J. 1990, Galactic and Intergalactic Magnetic Fields. Proceedings of the 140th. Symposium of the International Astronomical Union, held in Heidelberg, eds. Beck R., Kronberg P.P., Wielebinski R.; Publisher, Kluwer Academic Publishers, Dordrecht, The Netherlands; Boston, 383
Scoville N.Z. 1972, Ap. J. Lett. 175:L 127-32
Serabyn E., Lacy J.H. 1985, ApJ 293, 445
Serabyn E., Lacy J.H., Townes C.H., Bharat R. 1988, ApJ 326, 171
Serabyn E., Lacy J.H., Achtermann J.M. 1991, ApJ 378, 557
Sjouwerman L.O. 1997, The OH/IR star population in the Galactic center, PhD Thesis, Technical Report No. 316 (Chalmers University of Technology)
Sjouwerman L.O., van Langevelde H.J., Winnberg A., Habing H.J. 1998, A&AS 128, 35 (S-98)
Werner M.W., Davidson J.A., Morris M., Novak G., Platt S.R., Hildebrand R.H. 1988, ApJ 333, 729
Whiteoak J.B., Gardner F.F. 1975, MNRAS, 173, 25
Whiteoak J.B., Gardner F.F. 1976, MNRAS, 174, 627
Wilson T.L., Ruf K., Walmsley C.M., Martin R.N., Pauls T.A., Batrla W. 1982, A&A 15, 185
Winnberg A., 1984, Det Interstellära Mediet (Chalmers University of Technology)
Yusef-Zadeh F., Morris M. 1987 ApJ 320, 545
Yusef-Zadeh F., Morris M. 1991, ApJ 371, 59
Yusef-Zadeh F., Wardle M. 1992, The center, bulge, and disk of the Milky Way. ed. Blitz L. Dordrecht: Kluwer, Astrophysics and Space Science Library, 180, 1
Yusef-Zadeh F. 1998, GCNEWS - Galactic Center Newsletter, eds. Cotera A., Falcke H. 8, 3
Yusef-Zadeh F., Goss W.M., Roberts D.A., Robinson B., Frail D.A. 1999 ApJ 27, 172
Zhao J-H., Goss W.M., Ho T.P. 1995, ApJ 450, 122
Zylka R., Mezger P.G., Wink J.E. 1990, A&A 234, 133
Zylka R., Mezger P.G., Ward-Thompson D., Duschl W.J., Lesch H. 1995, A&A 297, 83
Zylka R. 1996, Kinematics of the Sgr A Cloud Complex, in the Galactic Center, ed. R. Gredel, ASP Conf. Ser. Vol. 102, 77

Paper I

THE 18-CM OH DISTRIBUTION IN THE GALACTIC CENTER TORUS

Aage Sandqvist and Roland Karlsson
Stockholm Observatory
S-133 00 Saltsjöbaden, Sweden

John B. Whiteoak and Frank F. Gardner
CSIRO, P.O. Box 76
Epping NSW 2121, Australia

ABSTRACT

The 18-cm OH distribution in the Galactic Center region near Sgr A has been studied in all four of the 1612, 1665, 1667 and 1720 MHz OH lines using the VLA with 4 arcsec angular resolution and 9 km s^{-1} velocity resolution. Three 1667 MHz OH spectral line absorption maps, at +51, +25 and -1 km s^{-1}, covering a 4'.3 x 4'.3 region around Sgr A are presented together with an 18-cm continuum map. In addition, a complete set of velocity maps from +139 to -159 km s^{-1}, covering a 3' x 3' region around the Galactic Center nuclear torus, is presented. Absorption by the +50 and +20 km s^{-1} molecular cloud belt is seen towards Sgr A East, but not towards Sgr A West. Absorption is also seen towards Sgr A* in the velocity ranges of +43 to -36 km s^{-1} and -142 to -151 km s^{-1}. The Northeast and Southwest torus components can be traced out to velocities of +139 and -151 km s^{-1}. A "Northwest" feature, starting northwest of the Western continuum arc, appears faintly at a velocity of +51 km s^{-1} and then migrates slightly southward until it merges with another feature at a velocity of +78 km s^{-1}. This other feature "Sweeps" in towards Sgr A* as the velocity decreases from +78 to +16 km s^{-1}.

INTRODUCTION AND OBSERVATIONS

Previous high resolution maps of OH towards Sgr A were obtained by the lunar occultation series in 1968 (Figure 1). They revealed that the continuum source is surrounded by a rotating and contracting cloud of dust and molecules (Sandqvist 1974)[1]. The infrared structure of this torus cloud was described in 1982 by Becklin, Gatley and Werner[2], while its kinematics was further discussed by Lester et al.[3] in 1981, Genzel et al.[4] in 1982 and Liszt, Burton and van der Hulst[5] in 1985. The "missing" Southeast molecular arm of the torus was detected and mapped with the rest of the torus in the J=3-2 HCO^+ line by Sandqvist, Wootten and Loren[6] in 1985.

We have studied the 18-cm OH distribution in the Galactic Center region near Sgr A in all four of the 1612, 1665, 1667 and 1720 MHz OH lines using the VLA in the A/B configuration. The observations were made on June 25 and 30, 1986 using 18 antennas and 64 frequency channels. The angular resolution in the 25' field of view is 4 arcsec, the channel frequency separation is 48.828 kHz resulting in a velocity resolution of about 9 km s^{-1} over a velocity range of about +/-280 km s^{-1}. The data was calibrated at the VLA using standard routines.

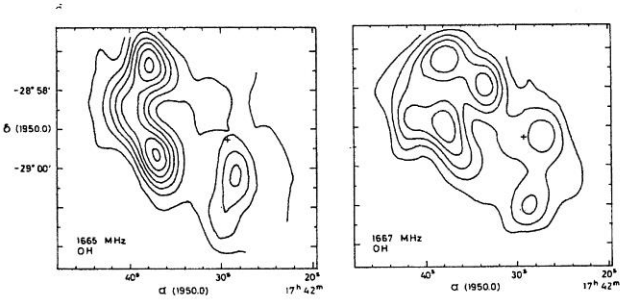

Figure 1. The velocity-integrated (-42 to +102 km s^{-1}) OH distribution (N_{OH}/T_{ex}). The cross marks the position of Sgr A*. (Sandqvist 1974)[1]

RESULTS AND DISCUSSION

Figure 2 shows three selected velocity channel maps (at +51, +25 and -1 km s^{-1}) covering the continuum region, which is also shown. The data has been hanned and the continuum map cleaned (Högbom 1974[7] and private communication). The outermost contour level in the spectral line aborption maps is -20 mJy/beam and the contour interval is -20 mJy/beam. For the continuum map, these values are 5 and 10 mJy/beam, respectively.

It is apparent from this figure that the gas in the +50 and +20 km s^{-1} molecular belt is seen clearly in absorption against the shell structure of Sgr A East but not against the spiral structure of Sgr A West. This may imply that the molecular belt lies between the two continuum components, behind Sgr A West and in front of Sgr A East.

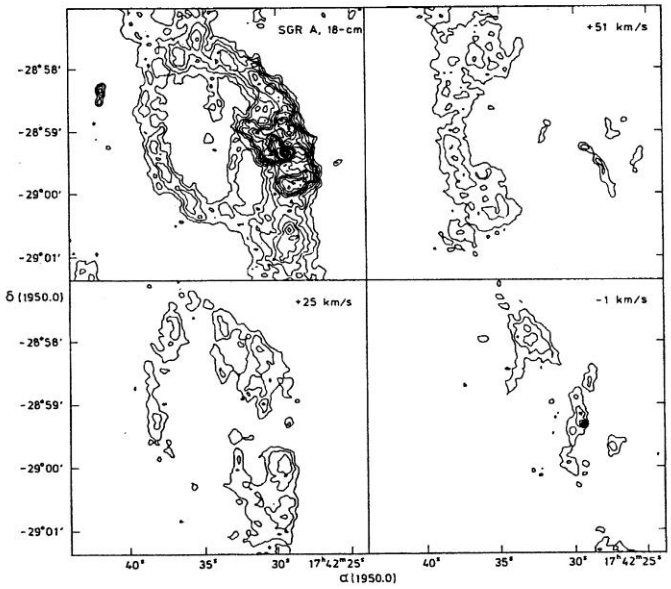

Figure 2. 1667 MHz OH spectral line absorption maps at +51, +25 and -1 km s^{-1}, and the 18-cm continuum map of Sgr A.

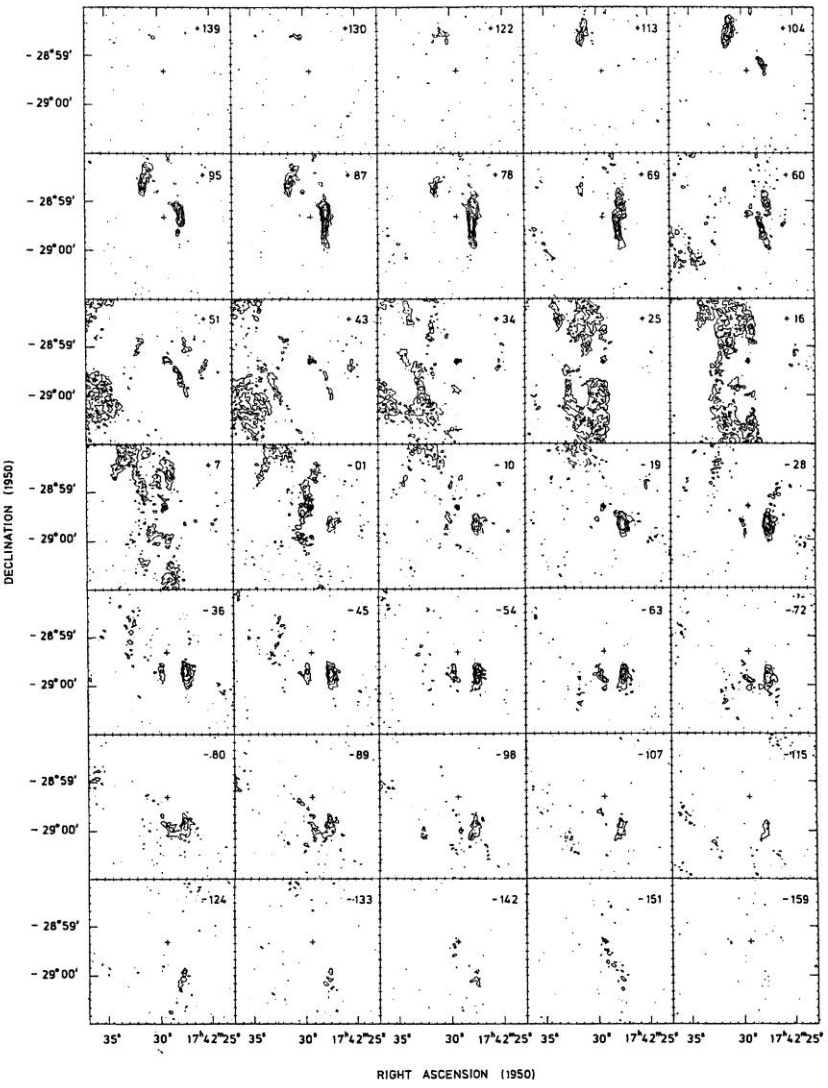

Figure 3. The 1667 MHz OH spectral line absorption maps. The radial velocity is given in the upper right hand corner. The cross marks the position of Sgr A*. The outermost contour level is -25 mJy/beam and the contour interval is -20 mJy/beam.

Yusef-Zadeh and Morris (1986)[8] have also presented evidence that Sgr A East lies behind Sgr A West. On the other hand, Whiteoak, Pankonin and Gardner (1983)[9] did find H_2CO absorption against Sgr A West at velocities of +41.5 to +49 km s^{-1}, so the picture is still not perfectly clear.

Figure 3 presents the 1667 MHz OH spectral line absorption maps of the nuclear torus region in the velocity range of +139 to -159 km s^{-1}. The outermost contour level is -25 mJy/beam and the contour interval is -20 mJy/beam. The angular resolution is 4 arcsec. A cross marks the position of Sgr A*; the radial velocity with respect to the local standard of rest is given in the upper right hand corner.

The Northeast and Southwest OH components, seen in the occultation maps, are very clear in the VLA maps. They can be traced out to velocities of +139 and -151 km s^{-1}, respectively. The signature of a rotating torus structure is especially clear in maps at velocities ranging from -63 to -98 km s^{-1}. Two new features, probably related to the torus but with distinct positive radial velocity components, can also be clearly identified. A "Northwest" feature, starting northwest of the Western continuum arc, appears faintly at a velocity of +51 km s^{-1} and then migrates slightly southwards until it merges with another feature at a velocity of +78 km s^{-1}. This other feature "Sweeps" in towards Sgr A*, in a most tantalizing manner, as the velocity decreases from +78 to +16 km s^{-1}. Finally, OH absorption is seen towards Sgr A* at all velocities in the ranges of +43 to -36 km s^{-1} and -142 to -151 km s^{-1}. Whiteoak, Gardner and Pankonin[9] found H_2CO absorption towards Sgr A* near 0 km s^{-1} but not between +40 and +50 km s^{-1}, whereas Liszt et al. (1983)[10] found HI in absorption towards Sgr A* at velocities between +40 and +60 km s^{-1}. The OH lines may give a more complete representation of the velocity extent of the gas absorption seen towards Sgr A*.

REFERENCES

1. Aa. Sandqvist, Astron. Astrophys. **33** , 413 (1974).
2. E. E. Becklin, I. Gatley and M. W. Werner, Astrophys. J. **258** 134 (1982).
3. D. F. Lester, M. W. Werner, J. W. V. Storey, D. M. Watson and C. H. Townes, Astrophys. J. (Letters) **248** , L109 (1981).
4. R. Genzel, D. M. Watson, C. H. Townes, D. F. Lester, H. L. Dinerstein, M. W. Werner and J. W. V. Storey, The Galactic Center, eds. G. Riegler and R. Blanford (American Institute of Physics, N. Y., 1982), p. 72.
5. H. S. Liszt, W. B. Burton and J. M. Van der Hulst, Astron. Astrophys. **142** , 237 (1985).
6. Aa. Sandqvist, A. Wootten and R.B. Loren, Astron. Astrophys. **152** , L25 (1985).
7. J. A. Högbom, Astron. Astrophys. Suppl. **15** , 417 (1974).
8. F. Yusef-Zadeh and M. Morris, Astrophys. J., Preprint (1986).
9. J. B. Whiteoak, F. F. Gardner and V. Pankonin, Mon. Not. Roy. Astron. Soc. **202** , 11P (1983).
10. H. S. Liszt, J. M. van der Hulst, W. B. Burton and M. Ondrechen, Astron. Astrophys. **126** , 341 (1983).

Paper II

OH IN THE ENVIRONMENT OF SGR A

Aa. SANDQVIST, R. KARLSSON and J. B. WHITEOAK
Stockholm Observatory *CSIRO, P.O. Box 76*
S-133 36 Saltsjöbaden, Sweden *Epping, NSW 2121, Australia*

ABSTRACT. The 18-cm distribution of OH in the Galactic Center region near Sgr A has been mapped in all four of the 1612, 1665, 1667 and 1720 MHz OH absorption lines using the VLA with 4 arcsec angular resolution and 9 kms^{-1} velocity resolution. The OH gas at +50 and +20 kms^{-1} is seen clearly in absorption against the shell structure of Sgr A East but not against the spiral structure of Sgr A West, possibly implying that this molecular gas lies between the two continuum components - behind Sgr A West and in front of Sgr A East. Inside the Circumnuclear Disk, there is a new neutral streamer which sweeps from the disk in towards Sgr A* as the observed radial velocity decreases from +78 to +16 kms^{-1}. The streamer may have a negative-velocity counterpart on the opposite side of Sgr A*.

1. OH and the Sgr A Complex

OH appears to surround the Sgr A continuum complex and has its highest concentration just outside the eastern rim of the Sgr A East shell . This was discovered by the lunar occultations of 1968, which also showed clear evidence of OH in the northeastern and southwestern components of the Circumnuclear Disk (CND) (Sandqvist 1974, *A. Ap.* 33, 413). Our VLA observations of the four 18-cm OH lines, with an angular resolution of 4", show that the molecular gas at the velocities of +50 and +20 km s^{-1} is seen in absorption against the eastern and western rims of the Sgr A East shell (Sandqvist et al. 1987, *The Galactic Center*, AIP Proc. Conf. 155, 95). There is, however, no evidence of absorption against Sgr A West. This would imply that Sgr A West is in front of, and Sgr A East behind, the distributed molecular gas. Many of the clumps and features seen in the HCN map of the CND made by Güsten et al. (1987, *The Galactic Center*, AIP Conf. Proc. 155, 103) can also be identified in our OH maps, and the disk's rotation signature can be traced out to +139 km s^{-1} in the northeast component and -151 km s^{-1} in the southwest.

2. The Sgr A* 1667-MHz OH Streamer

We have detected a new molecular gas streamer *inside* the CND which stretches from the disk's southwestern region inwards through the "empty" cavity to the compact non-themal radio source, Sgr A*. This OH streamer is shown in a series of

M. Morris (ed.), The Center of the Galaxy, 421–422.

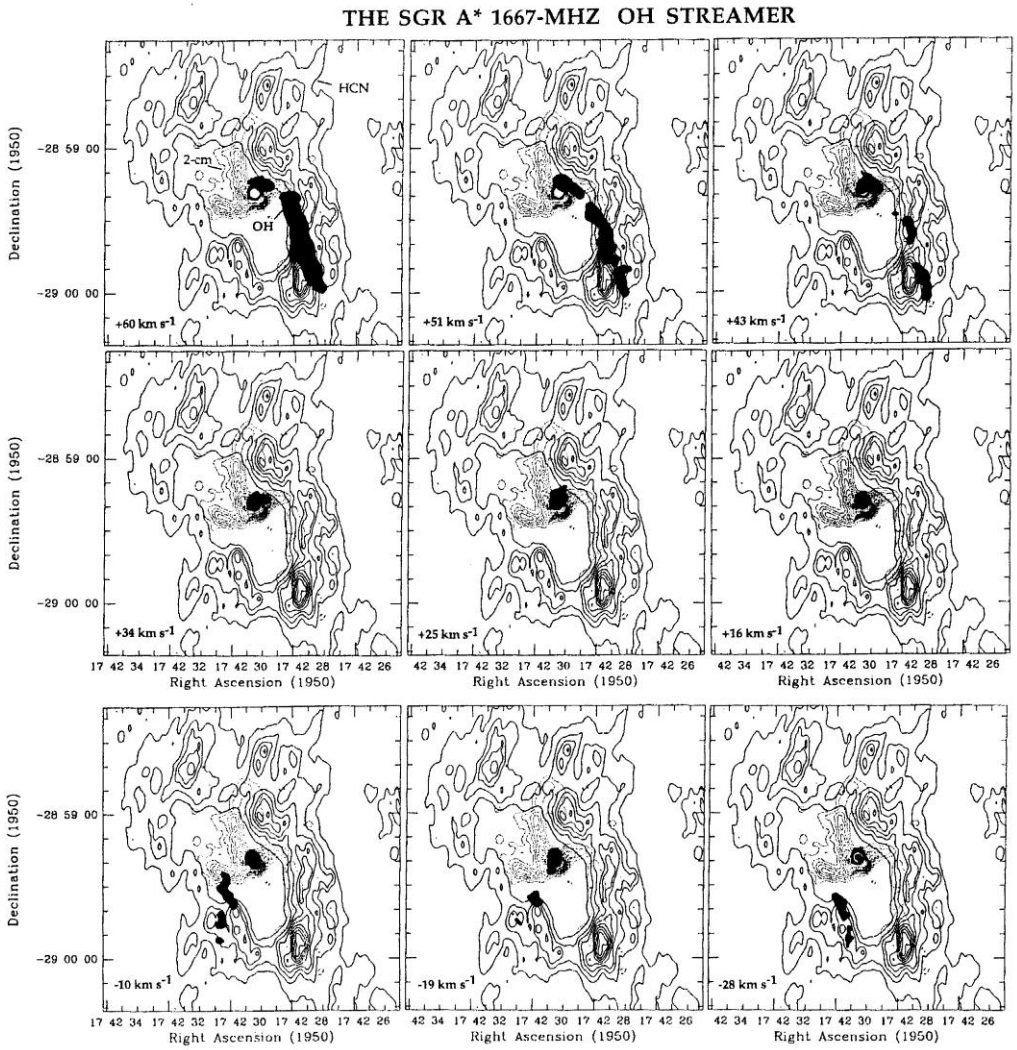

velocity maps in the figure and superimposed upon the HCN map of Güsten et al. and the 2-cm continuum map of Ekers et al. (1983, *A. Ap.*. 122, 143). At a velocity of +60 km s^{-1} the streamer cuts across the southwestern part of the CND. Note that the negative velocity of the CND in this region differs from that of the streamer by more than 100 km s^{-1} , and the streamer may not necessarily be in the same plane as the CND. The OH streamer moves closer to Sgr A* as the velocity drops until at +16 km s^{-1} it coincides with Sgr A*. The streamer may have a counterpart on the southeastern side of Sgr A* at negative velocities (-10 to -28 km s^{-1}). We have not included the map at -1 km s^{-1} due to possible contamination by unrelated foreground gas, but we refer the interested reader to Fig. 3 of Sandqvist et al. (1987).

It is difficult to understand how the OH streamer can survive in the strong UV radiation field in the cavity inside the CND but the OH may be protected to some extent if it is intermingled with dust. There may indeed be some evidence for such a dust streamer in the same position as the OH streamer, and its possible counterpart, in the near infrared extinction (H-K) map presented by Gatley, Depoy and Fowler at this symposium.

Paper III

Paper IV

Appendix

References

Aitken D.K., Smith C.H., Roche P.F., Wright C.M. 1990, MNRAS 246, 1
Armstrong J.T., Barrett A.H. 1985, ApJS, 57, 535
Avrett E.H. 1979, ed. Frontiers of Astrophysics
Balick B., Brown R.L. 1974, ApJ 194, 265
Begelman M.C., Frank J., Shlosman I., 1989, Theory of Accretion Disks, eds. F. Meyer, W.J. Duschl, J. Frank, E. Meyer-Hofmeister, Proceedings of a NATO Advanced Research Workshop, held in Garching, Dordrecht: Kluwer 290, 373
Bieging J.H. 1976, A&A 51, 289
Binney J., Gerhard O.E., Stark A.A., Bally J., Uchida K.I. 1991, MNRAS 252, 210B
Bower G.C., Falcke H., Backer D.C. 1999, 195th AAS Meeting, Bulletin of the American Astronomical Society 31, 1463
Bower G.C. 2000, GCNEWS 11, 4, eds. Cotera A., Falcke H., Markoff S.
Boyce P.J., Cohen R.J. 1994, A&AS 107, 563
Brown R.L., Johnston K.J., Lo K.Y. 1981, ApJ 250, 155
Brown R.L., Lo K.Y. 1982, ApJ 253, 108
Coil A.L., Ho P.T.P. 2000, ApJ 533, 245
Coker R., Melia F. 1997, ApJ 488, 149
Cornwell T. 1982, NRAO/VLA WORKSHOP: SYNTHESIS MAPPING, 9
Duschl W. J., Lesch H. 1994, A&A 286, 431
Eckart A., Genzel R., Hofmann R., Sams B.J., Tacconi-Garman L.E. 1993, ApJ 407, 77
Eckart A., Genzel R. 1996, Nature 383, 415
Eckart A., Genzel R. 1997, MNRAS 284, 576
Ekers, R.D. 1982, Synthesis Mapping, Proc of the NRAO-VLA Workshop Socorro, iv
Ekers R.D., van Gorkom J.H., Schwarz U.J., Goss W.M. 1983, A&A 122, 143
Frail D.A., Goss W.M., Slysh V.I., 1994, ApJ 424, L111
Gatley I., Beattie D.H., Lee T.J., Jones T.J., Hyland A.R. 1984, MNRAS 210, 565
Gatley I., Jones T.J., Hyland A.R., Wade R., Geballe T.R. 1986, MNRAS 222, 299
Geballe T.R., Krisciunas K., Lee T.J., Gatley I., Wade R., Duncan W.D., Garden R., Becklin E. E. 1984, ApJ 284, 118
Geballe T.R., Wade R., Krisciunas K., Gatley I., Bird M.C. 1987, ApJ 320, 562
Genzel R., Townes C.H. 1987, ARAA 25, 377
Genzel R., Stacey G.J., Harris A.I., Townes C.H., Geis N. 1989, IAU-Symp 136, 151
Genzel R., Stacey G.J., Harris A.I., Townes C.H., Geis N., Graf U.U., Poglitsch A., Stutzki J. 1990, ApJ 356, 160
Genzel R., Hollenbach D., Townes C.H. 1994, Rep. Prog. Phys. 57, 417
Genzel R., Thatte N., Krabbe A., Kroker H., Tacconi-Garman L.E. 1996, ApJ 472, 153
Gerhard O.E., Stark A.A., Bally J., Uchida K.I. 1991, MNRAS 252, 210
Ghez A.M., Klein B.L., Morris M., Becklin E.E. 1998, ApJ 509, 678
Ghez A.M., Morris M., Becklin E.E., Tanner A., Kremenek T. 2000, Nature 407, 349
Güsten R., Downes D. 1981, A&A 99, 27
Güsten R., Walmsley C.M., Pauls T. 1981, A&A 103, 197
Güsten R., Genzel R., Wright M.C.H., Jaffe D.T., Stutzki J., Harris A.I. 1987, ApJ 318, 124
Hall D.N.B., Kleinmann S.G., Scoville N.Z. 1982, ApJ 260, 53
Hauser M.G., Kelsall T., Leisawitz D., Weiland J. 1995, COBE DIRBE Explanatory Supplement Vers. 2.0, COBE Ref. Pub. No. 95-A (Greenbelt, MD: NASA/GSFC)

Hildebrand R.H., Gonatas D.P., Platt S.R., Wu X.D., Davidson J.A., Werner M.W., Novak G., Morris M. 1990, ApJ 362, 114
Högbom J. 1974, A&AS 15, 417
Högbom, ~ 1985, Bildprogram för Finsmakare, BIFF, Stockholms Observatorium
Hüttemeister S., Wilson T.L., Bania T.M., Martin-Píntado J. 1993 A&A 280, 255
Jackson J.M., Geis N., Genzel R., Harris A.I., Madden S., Poglitsch A., Stacey G.J., Townes C.H. 1993, ApJ 402, 173
Kaifu N., Kato T., Iguchi T. Nature 1972, 238, 105
Karlsson R., Sandqvist Aa., Sjouwerman L.O., Whiteoak J.B. 2003 Paper III, Astronomische Nachrichten/AN, Suppl. Issue 1/2003
Karlsson R., Sjouwerman L.O., Sandqvist Aa., Whiteoak J.B. 2003 Paper IV, A&A 403, 1011
Killeen N.E.B., Lo K.Y., Crutcher R.1992, ApJ 385, 585
Koyama K., Awaki H., Kunieda H., Takano S., Tawara Y. 1989, Nature 339, 603
Koyama K., Maeda Y. 1996, IAUS 169, 287
Krichbaum T.P., Graham D.A., Witzel A., Greve A., Wink J.E., Grewing M., Colomer F., de Vicente P., Gomez-Gonzalez J., Baudry A., Zensus J.A.1998, A&A 335, 106
Lacy J.H., Townes C.H., Geballe T.R., Hollenbach D.J. 1980, ApJ 241, 132
Lebofsky M.J., Rieke G.H., Deshpande M.R., Kemp J.C. 1982, ApJ 263, 672
Lindqvist M., Winnberg A., Habing H.J., Matthew H.E. 1992, A&AS 92, 43 (L-92)
Lo K.Y., Claussen M.J. 1983, Nature 306, 647
Lynden-Bell D., Rees M.J. 1971, MNRAS 152, 461
Marshall J., Lasenby A. 1994, in: The nuclei of normal galaxies – Lessons from the Galactic Center, eds. Genzel and Harris, 175
Melia F., Falcke H. 2001, Annu. Rev. Astron. Astrophys. 39, 309
Menten K.M., Reid M.J., Eckart A. 1997, ApJ 475, 111
Mezger P.G., Zylka R., Salter C.J., Wink J.E., Chini R., Kreysa E., Tuffs R. 1989, A&A 209, 337
Mezger P.G., Duschl W.J., Zylka R. 1996, A&A 7, 289
Morris M., Serabyn E. 1996, Annu. Rev. Astron. Astrophys. 34, 645
Palmer P., Goss W.M. 1996, GCNEWS - Galactic Center Newsletter, eds. A. Cotera & H. Falcke 2, 3
Piddington J.H., Minnett H.C. 1951, Aust. J. Sci. Res. A 4, 459
Pihlström Y.M., Conway J.E., Booth R.S., Diamond P.J., Polatidis A.G. 2001, A&A 377, 413
Poglitsch A., Stacey G.J., Geis N., Haggerty M., Jackson J., Rumitz M., Genzel R., Townes C.H. 1991, ApJ 374, 33
Predehl P., Trümper J. 1994, A&A 290, 29
Readhead A.C.S. 1994, ApJ 426, 51
Reid M. J. 1993, Annu. Rev. Astron. Astrophys. 31, 345
Roberts D.A., Yusef-Zadeh F., Goss W.M. 1966 ApJ 459, 627
Robinson D.A., McGee R.X. 1970, Austr. J. Phys. 23, 405
Rogers A.E.E., Doelman S., Wright M.C.H., Bower G.C., Geoffrey C., Backer D.C., Padin S., Philips J.A., Emerson D.T., Greenhill L., Moran J.M., Kellermann K.I. 1994 ApJ 434, 59
Sanders D.B., Scoville N.Z., Solomon P.M. 1985, ApJ 289, 373
Sandqvist Aa. 1971, Lunar Occultations of the Galactic Center Region in HI, OH and CH2O Lines, PhD Thesis (University of Maryland)
Sandqvist Aa. 1973, A&AS 9, 391
Sandqvist Aa. 1974, A&A 33, 413
Sandqvist Aa. 1989, A&A 223, 293

Sandqvist Aa., Karlsson R., Whiteoak J.B. 1989, OH in the Environment of Sgr A, in IAU Symp 136, The Center of the Galaxy, ed. M. Morris (Kluwer, Dordrecht), 421
Sandqvist Aa., Karlsson R., Whiteoak J.B., Gardner F.F. 1987, The 18-cm OH Distribution in the Galactic Center Torus, in AIP Conf. Proc. 155, The Galactic Center, ed. D.C. Backer (AIP, New York), 95
Schödel R., Ott T., Genzel R., Hofmann R., Lehnert M., Eckart A., Mouawad N., Alexander T., Reid M.J., Lenzen R., Hartung M., Lacombe F., Rouan D., Gendron E., Rousset G., Lagrange A.-M., Brandner W., Ageorges N., Lidman C., Moorwood A.F.M., Spyromilio J., Hubin N., Menten K.M. 2002, Nature 419, 694
Schwarz U.J., Bregman J.D., van Gorkom J.H. 1989, A&A 215, 33
Schwarz U.J., Lasenby J. 1990, Galactic and Intergalactic Magnetic Fields. Proceedings of the 140th. Symposium of the International Astronomical Union, held in Heidelberg, eds. Beck R., Kronberg P.P., Wielebinski R.; Publisher, Kluwer Academic Publishers, Dordrecht, The Netherlands; Boston, 383
Scoville N.Z. 1972, Ap. J. Lett. 175:L 127-32
Serabyn E., Lacy J.H. 1985, ApJ 293, 445
Serabyn E., Lacy J.H., Townes C.H., Bharat R. 1988, ApJ 326, 171
Serabyn E., Lacy J.H., Achtermann J.M. 1991, ApJ 378, 557
Sjouwerman L.O. 1997, The OH/IR star population in the Galactic center, PhD Thesis, Technical Report No. 316 (Chalmers University of Technology)
Sjouwerman L.O., van Langevelde H.J., Winnberg A., Habing H.J. 1998, A&AS 128, 35 (S-98)
Werner M.W., Davidson J.A., Morris M., Novak G., Platt S.R., Hildebrand R.H. 1988, ApJ 333, 729
Whiteoak J.B., Gardner F.F. 1975, MNRAS, 173, 25
Whiteoak J.B., Gardner F.F. 1976, MNRAS, 174, 627
Wilson T.L., Ruf K., Walmsley C.M., Martin R.N., Pauls T.A., Batrla W. 1982, A&A 15, 185
Winnberg A., 1984, Det Interstellära Mediet (Chalmers University of Technology)
Yusef-Zadeh F., Morris M. 1987 ApJ 320, 545
Yusef-Zadeh F., Morris M. 1991, ApJ 371, 59
Yusef-Zadeh F., Wardle M. 1992, The center, bulge, and disk of the Milky Way. ed. Blitz L. Dordrecht: Kluwer, Astrophysics and Space Science Library, 180, 1
Yusef-Zadeh F. 1998, GCNEWS - Galactic Center Newsletter, eds. Cotera A., Falcke H. 8, 3
Yusef-Zadeh F., Goss W.M., Roberts D.A., Robinson B., Frail D.A. 1999 ApJ 27, 172
Zhao J-H., Goss W.M., Ho T.P. 1995, ApJ 450, 122
Zylka R., Mezger P.G., Wink J.E. 1990, A&A 234, 133
Zylka R., Mezger P.G., Ward-Thompson D., Duschl W.J., Lesch H. 1995, A&A 297, 83
Zylka R. 1996, Kinematics of the Sgr A Cloud Complex, in the Galactic Center, ed. R. Gredel, ASP Conf. Ser. Vol. 102, 77